

Synthetic Heterogeneous-Effects LASSO: A Fixed-effects Estimation Approach for High-dimensional Mixed-effects Models

Shangyuan Ye*, Cong Zhang[†], Ying Chen[‡], Ye Liang[§], and Guanbo Wang[¶]

Abstract

This paper studies variable selection and post-selection inference for high-dimensional clustered data using marginal-model-based procedures. We show that, when covariates are heterogeneously distributed across clusters, marginal-model LASSO may use them as sparse proxies for latent cluster effects, shifting the estimation target away from the structural fixed effects and inducing false selections. To address this problem, we propose Synthetic Heterogeneous-Effects LASSO (SHEL), a fixed-effects penalized framework that incorporates cluster-level synthetic approximations to the latent heterogeneity. We establish theoretical properties of SHEL in high-dimensional settings and develop procedures for valid post-selection inference. The finite sample performance of the proposed method is investigated through extensive simulation studies. A longitudinal bulk RNA-seq dataset of enriched blood neutrophils from hospitalized COVID-19 patients is analyzed to demonstrate the method in a real application.

Keywords: High-dimensional data; Clustered data analysis; Target shift; Synthetic approximation.

*Shangyuan Ye is Assistant Professor in the Department of Mathematics and Statistics at Florida International University, Miami, FL, U.S.A. (e-mail: sye@fiu.edu)

[†]Cong Zhang is Principal Biostatistician in the China Novartis Institutes for Bio-Medical Research Co, Shanghai, China (e-mail: zhcong.pku@gmail.com)

[‡]Ying Chen is Instructor in the Department of Statistics and Data Science, University of Pennsylvania, Philadelphia, PA, U.S.A. (e-mail: chen136@wharton.upenn.edu)

[§]Ye Liang is Associate Professor in the Department of Statistics at Oklahoma State University, Stillwater, OK, U.S.A. (e-mail: ye.liang@okstate.edu)

[¶]Guanbo Wang is Assistant Professor in the Dartmouth Institute for Health Policy and Clinical Practice, Geisel School of Medicine, Dartmouth College, Hanover, NH, U.S.A. (e-mail: guanbo.wang@dartmouth.edu).

1 Introduction

Clustered data, where subjects can be grouped into different clusters or groups, are common in many fields such as sociology, biomedicine, and health services research. Although numerous traditional methods have been developed to address the multilevel structure in low-dimensional clustered data analysis, problems with high-dimensionality present novel challenges in parameter estimation and inference.

In high-dimensional settings, variable selection and statistical inference for correlated data are more challenging than those for independent data. Existing approaches consider either high-dimensional generalized linear mixed-effects models (GLMM) (Fan and Li, 2012; Li et al., 2015; Hui et al., 2017) or high-dimensional marginal models fit through generalized estimation equations (GEE) (Xu et al., 2010; Wang et al., 2012; Chen et al., 2026), both of which then incorporate a regularization-based method, such as LASSO (Tibshirani, 1996) or SCAD (Fan and Li, 2001).

Statistical inference using likelihood-based approaches for mixed-effects models can be substantially more complicated than inference for independent data. In particular, GLMM likelihood functions generally require numerical integration over the random effects, and such approximations can be computationally intensive with high dimensionality (Tutz and Groll, 2013; Ye et al., 2025b). Post-selection inference adds another layer of difficulty. Existing approaches include data splitting (Rinaldo et al., 2019), simultaneous inference (Berk et al., 2013), and selective inference (Lee et al., 2016). Kuchibhotla et al. (2022) provides a comprehensive review of post-selection inference methods. In clustered data, naive observation-level splitting may violate the required independence between the selection sample and the inference sample. Simultaneous inference can be conservative in sparse high-dimensional settings. Selective inference provides a more targeted approach by conditioning on the selected model, but its extension to mixed-effects models remains limited. Existing

selective inference methods are mainly developed for fixed-design Gaussian regression or low-dimensional likelihood-based models, where the selection event or score process is tractable (Lee et al., 2016; Taylor and Tibshirani, 2018). For high-dimensional LMM, existing procedures have not shown satisfactory performance (D’Alessandro and Thoresen, 2025). For GLMM, although penalized estimation and variable selection methods are available (Fan and Li, 2012; Hui et al., 2017; Heiling et al., 2024), their focus is primarily on estimation and selection rather than valid inference after selection.

Marginal-model-based approaches provide an attractive alternative for analyzing clustered data because they do not require correct specification of the within-cluster correlation structure to yield valid inference for marginal model parameters. As fixed-effects approaches, they are also computationally more feasible than the likelihood-based methods for high-dimensional GLMM. However, previous studies have shown that marginal-model-based variable selection procedures may include a large proportion of falsely selected variables (Ye et al., 2025a; Muff et al., 2016). The theoretical explanation of this phenomenon is studied in Section 2 of this paper. In particular, when some covariates are heterogeneously distributed across clusters, a penalized estimator uses them as proxies for latent cluster effects, either through a genuine dependence or through spurious sample correlations in high-dimensional settings. Although such proxies can improve prediction, they may distort variable selection and post-selection inference by shifting the estimation target away from the structural fixed effects. We formalize this target-shift phenomenon in a theory and show that, when the cluster effects admit an approximately sparse representation through cluster-level covariate summaries, the marginal model LASSO converges to a biased target that combines the true fixed effects with a sparse proxy for the latent intercepts.

Motivated by the theory, we propose the Synthetic Heterogeneous-Effects LASSO (SHEL), a computationally tractable fixed-effects penalized framework for estimation and inference

in high-dimensional mixed-effects models. The proposed SHEL explicitly constructs cluster-constant synthetic approximations to the latent heterogeneous effects and penalizes them jointly with the original covariates. This strategy reduces the tendency of high-dimensional penalized estimators to select scientifically irrelevant covariates as surrogates for the latent cluster heterogeneity while preserving the computational simplicity of the LASSO-type methods. As a fixed-effects-based approach, SHEL retains theoretical properties analogous to those of the standard LASSO, which allows existing post-selection inference ideas, such as selective inference (Lee et al., 2016) and debiased LASSO (Van de Geer et al., 2014), to be adapted. Specifically, we develop polyhedral selective inference for linear SHEL and a debiased GSHEL procedure for generalized linear models, with the latter one accounting for cluster-level dependence through a cluster-level central limit theorem.

The remainder of the paper is organized as follows. Section 2.2 studies the target-shift phenomenon. Section 2.3 introduces the proposed SHEL estimator for LMM, and Section 2.4 establishes its theoretical properties. Section 3 extends the method to GLMM. Sections 4.1 and 4.2 present polyhedral selective inference for SHEL and debiased inference for GSHEL, respectively. Section 5 describes the implementation details. Section 6 evaluates the finite-sample performance of the proposed methods through simulation studies, and Section 7 applies the method to a longitudinal bulk RNA-seq dataset. Section 8 concludes with a discussion.

2 Synthetic heterogeneous-effects LASSO

2.1 Model and notation

Let Y_{ij} denote the response variable of the j th individual in the i th cluster, and \mathbf{X}_{ij} denote the corresponding p -dimensional vector of covariates with $i \in \{1, \dots, m\}$, $j \in \{1, \dots, n_i\}$,

and $N = n_1 + \dots + n_m$. We consider the generalized linear heterogeneous-intercepts model, where the conditional distribution of Y_{ij} given \mathbf{X}_{ij} belongs to an exponential family:

$$f(y_{ij}; \mu_{ij}) = \exp\{y_{ij}g(\mu_{ij}) - b(\mu_{ij}) + c(y_{ij})\}, \quad \xi_{ij} = g(\mu_{ij}) = \mathbf{X}_{ij}^\top \boldsymbol{\beta}^0 + \alpha_i, \quad (1)$$

where $\boldsymbol{\beta}^0$ is a p -vector of fixed effects, $\boldsymbol{\alpha} = (\alpha_1, \dots, \alpha_m)^\top$ is a m -vector of cluster-specific intercepts, and $b(\cdot)$ and $c(\cdot)$ are known functions.

We start with the linear heterogeneous-intercepts model, where (1) can be written as

$$Y_{ij} = \mathbf{X}_{ij}^\top \boldsymbol{\beta}^0 + \alpha_i + \epsilon_{ij}, \quad (2)$$

with ϵ_{ij} being independent sub-Gaussian random errors with mean 0 and sub-Gaussian norm bounded by a constant $\sigma > 0$, that is, $\|\epsilon_{ij}\|_{\psi_2} \leq \sigma$ for all i and j . Here, σ is a uniform upper bound on the tail magnitude of the within-cluster random errors. In high-dimensional settings, we assume that the true model is sparse, i.e., only a small number of β_l^0 , $l = 1, \dots, p$ values are non-zero. We denote $\mathcal{M}_1 = \text{supp}(\boldsymbol{\beta}^0)$, and $|\mathcal{M}_1| = M_1$. Let $\mathbf{D} \in \mathbb{R}^{N \times m}$ denote the cluster-indicator matrix, whose row corresponding to observation (i, j) has a 1 in the i th column and 0 elsewhere. Then the (i, j) -th entry of the vector $\mathbf{D}\boldsymbol{\alpha}$ is α_i , meaning that each observation in cluster i shares the same cluster-specific intercept. With this notation, the matrix form of model (2) is

$$\mathbf{Y} = \mathbf{X}\boldsymbol{\beta}^0 + \mathbf{D}\boldsymbol{\alpha} + \boldsymbol{\epsilon}. \quad (3)$$

2.2 The impact of heterogeneous effects on marginal model LASSO

The marginal version of the model (2) can be expressed as

$$Y_{ij} = \mathbf{X}_{ij}^\top \tilde{\boldsymbol{\beta}} + \tilde{\epsilon}_{ij}, \quad \tilde{\epsilon}_{ij} = \alpha_i + \epsilon_{ij}. \quad (4)$$

The marginal parameter $\tilde{\boldsymbol{\beta}}$ represents the population-average covariate effects (Zeger et al., 1988). For the linear model considered here, $\tilde{\boldsymbol{\beta}} = \boldsymbol{\beta}^0$. When p is fixed, generalized estimating equations (GEE) with a robust sandwich variance estimator are commonly used for inference on $\tilde{\boldsymbol{\beta}}$. In high-dimensional settings, penalized GEE (PGEE) has been proposed to perform variable selection and parameter estimation simultaneously (Wang et al., 2012).

Motivated by the marginal representation (4), we first evaluate the marginal-model LASSO estimator, which ignores the heterogeneous effects:

$$\hat{\boldsymbol{\beta}} = \arg \min_{\boldsymbol{\beta} \in \mathbb{R}^p} \left\{ \frac{1}{2N} \|\mathbf{Y} - \mathbf{X}\boldsymbol{\beta}\|_2^2 + \lambda \|\boldsymbol{\beta}\|_1 \right\}. \quad (5)$$

This estimator can be viewed as the analogue of a PGEE estimator under an independence working correlation structure, specialized to the Gaussian linear model setting.

Substituting (3) into (5) shows that the objective function is based on the full signal $\mathbf{X}\boldsymbol{\beta}^0 + \mathbf{D}\boldsymbol{\alpha}$, rather than only the target fixed-effects component $\mathbf{X}\boldsymbol{\beta}^0$. As a result, the fitted linear predictor $\mathbf{X}\hat{\boldsymbol{\beta}}$ may partially absorb variation due to the latent heterogeneous intercepts. Under the traditional assumption that the covariate distribution is homogeneous across clusters, the covariates carry no systematic information about $\mathbf{D}\boldsymbol{\alpha}$, so the marginal model LASSO still targets $\boldsymbol{\beta}^0$. More generally, in low-dimensional settings, if the cluster-level heterogeneity in \mathbf{X} is independent of $\boldsymbol{\alpha}$, the marginal estimator remains valid for $\boldsymbol{\beta}^0$.

The problem arises when the covariate distribution is heterogeneous across clusters and the dimensionality is high. In such cases, even under independence of \mathbf{X} and $\boldsymbol{\alpha}$, the large

number of covariates makes it increasingly likely that some heterogeneously distributed covariates exhibit spurious sample correlations with $\boldsymbol{\alpha}$. Consequently, the marginal-model LASSO can exploit this correlation and use a sparse subset of covariates to proxy for $\boldsymbol{\alpha}$. More precisely, since $\mathbf{D}\boldsymbol{\alpha}$ is a constant within each cluster, a sparse linear combination of the cluster means of X_l will be used to predict $\mathbf{D}\boldsymbol{\alpha}$.

To illustrate a technical explanation, we assume $X_{l,ij} = \mu_{l,i} + \xi_{l,ij}$, where $E(\xi_{l,ij}) = 0$. Let $\mathcal{P}_0 \subset \{1, \dots, p\}$ denote the index set of covariates whose cluster-specific means vary across clusters, that is, for each $l \in \mathcal{P}_0$, $\mu_{l,i}$ vary across i . Let $\mathbf{B}_c \in \mathbb{R}^{m \times p_0}$, with $p_0 = |\mathcal{P}_0|$, be the matrix whose (i, l) -th entry is the cluster mean $\mu_{l,i}$ for $l \in \mathcal{P}_0$. Define $\boldsymbol{\gamma}^*$ to be the best M_2 -sparse linear predictor of $\boldsymbol{\alpha}$ based on \mathbf{B}_c , namely,

$$\boldsymbol{\gamma}^* = \arg \min_{\boldsymbol{\gamma} \in \mathbb{R}^{p_0}, \|\boldsymbol{\gamma}\|_0 = M_2 m} \frac{1}{m} \|\boldsymbol{\alpha} - \mathbf{B}_c \boldsymbol{\gamma}\|_2^2.$$

Let $\boldsymbol{\beta}^* = \boldsymbol{\beta}^0 + \tilde{\boldsymbol{\gamma}}^*$, where $\tilde{\gamma}_l^* = \gamma_l^*$ when $l \in \mathcal{P}_0$, and 0 otherwise. Then model (2) can be expressed as

$$Y_{ij} = \mathbf{X}_{ij}^\top \boldsymbol{\beta}^* + (\alpha_i - \boldsymbol{\mu}_{ij}^\top \tilde{\boldsymbol{\gamma}}^*) + e_{ij} = \mathbf{X}_{ij}^\top \boldsymbol{\beta}^* + (\alpha_i - \boldsymbol{\mu}_{\mathcal{P}_0, ij}^\top \boldsymbol{\gamma}^*) + e_{ij}, \quad (6)$$

where $e_{ij} = \epsilon_{ij} - \boldsymbol{\xi}_{ij}^\top \tilde{\boldsymbol{\gamma}}^* = \epsilon_{ij} - \boldsymbol{\xi}_{\mathcal{P}_0, ij}^\top \boldsymbol{\gamma}^*$, $\|e_{ij}\|_{\psi_2} \leq \tilde{\sigma}$, and $\boldsymbol{\mu}_{ij}$ and $\boldsymbol{\xi}_{ij}$ denote the vectors of $\mu_{l,ij}$ and $\xi_{l,ij}$, respectively. Representation (6) highlights the effect of covariate heterogeneity: the term $\boldsymbol{\mu}_{ij}^\top \tilde{\boldsymbol{\gamma}}^*$ partially explains the latent intercept α_i , which can improve prediction, but it also shifts the target of estimation from the structural fixed-effects vector $\boldsymbol{\beta}^0$ to the contaminated coefficient vector $\boldsymbol{\beta}^*$. In addition, the extra term $\boldsymbol{\xi}_{ij}^\top \tilde{\boldsymbol{\gamma}}^*$ contributes additional residual variation.

Under regularity conditions given in the supplementary file, we derive the following theorem.

Theorem 1 Under the regularity conditions (C1)-(C4), let

$$\delta_m^2 = \frac{1}{m} \|\boldsymbol{\alpha} - \mathbf{B}_c \boldsymbol{\gamma}^*\|_2^2$$

and $M^* = \text{supp}(\boldsymbol{\beta}^*)$. When the tuning parameter λ satisfies $\lambda \geq \sqrt{16C\tilde{\sigma}^2 \log(p)/N}$ for some constant $C > 0$, we have

(I)

$$\frac{1}{N} \|\mathbf{X}(\hat{\boldsymbol{\beta}} - \boldsymbol{\beta}^*)\|_2^2 = O_p(\delta_m^2 + \lambda^2 M^*);$$

(II)

$$\|\hat{\boldsymbol{\beta}} - \boldsymbol{\beta}^*\|_1 = O_p(\sqrt{M^*} \delta_m + \lambda M^*);$$

(III) Let $r_{ij} = Y_{ij} - \hat{\boldsymbol{\beta}}^\top \mathbf{X}_{ij}$ denote the residual, and define the residual intracluster correlation coefficient (ICC) by

$$\rho_r = \frac{\text{Var}\{E(r_{ij} | i)\}}{\text{Var}(r_{ij})},$$

where $E(r_{ij} | i)$ is the cluster-specific mean of the residual. Then, for some constant $C' > 0$,

$$\rho_r \leq C' \frac{\delta_m^2 + \lambda^2 M^*}{\sigma^2 + \delta_m^2 + \lambda^2 M^*}.$$

A detailed proof is provided in the supplementary material. Theorem 1 confirms that the marginal model LASSO estimator (5) consistently estimates $\boldsymbol{\beta}^*$, rather than the targeted parameter $\boldsymbol{\beta}^0$, and the residual within-cluster correlation can be smaller than expected if δ_m^2 is small. Our next corollary, as a direct consequence of Theorem 1, formalizes the concept of

target shift induced by the across-cluster heterogeneity of the covariate distribution.

Corollary 1 *Under the conditions of Theorem 1, if $\sqrt{M^*} \delta_m + \lambda M^* = o(1)$, then*

$$\hat{\beta} - \beta^0 = \tilde{\gamma}^* + o_p(1).$$

This result explains the mechanism causing inflated false selections when using marginal-model LASSO for high-dimensional clustered data. When the high-dimensional covariates contain sufficient between-cluster information, a sparse linear combination of their cluster means can partially recover the latent cluster effects. In that case, even though the model is misspecified for fixed-effects estimation, (5) may still perform well for prediction. However, because it targets $\beta^* = \beta^0 + \tilde{\gamma}^*$ rather than β^0 , it may select variables that are predictive of the latent cluster effects rather than truly associated with the outcome through the structural fixed effects. Only in the special case where all covariates are homogeneously distributed across clusters does this contamination disappear, so that the cluster means carry no information about α and (5) is consistent for β^0 .

2.3 The SHEL estimator

To address the target-shift-induced estimation bias, we introduce the SHEL estimator. The key idea is to restrict LASSO from implicitly using selected covariates to approximate the latent intercepts. To do so, we explicitly construct cluster-level summary statistics to capture the between-cluster variation in α .

Let $\mathbf{b}_i \in \mathbb{R}^{p_0}$ denote a cluster-level summary vector for cluster i . For example, \mathbf{b}_i can be the cluster means of X_l for $l \in \mathcal{P}_0 \subset \{1, \dots, p\}$ or principal component scores of the cluster means. Based on these summary statistics, define a cluster-constant matrix $\mathbf{B} \in \mathbb{R}^{N \times p_0}$ such that the row of \mathbf{B} corresponding to observation (i, j) is \mathbf{b}_i^\top , for all $j = 1, \dots, n_i$. The role of \mathbf{B}

is not to recover the random intercepts exactly, but to provide a structured approximation to the latent cluster-level heterogeneity that might otherwise be spuriously absorbed by \mathbf{X} . By explicitly reserving a low-complexity component $\mathbf{B}\boldsymbol{\gamma}$ for cluster-level variations, the penalized fit can fix $\boldsymbol{\beta}$ on the covariate effects without being biased by the random effects proxies.

We therefore propose the following fixed-effects penalized estimator, or SHEL, to estimate $\boldsymbol{\beta}$ while using $\mathbf{B}\boldsymbol{\gamma}$ as a synthetic approximation to $\boldsymbol{\alpha}$:

$$(\hat{\boldsymbol{\beta}}, \hat{\boldsymbol{\gamma}}) = \arg \min_{\boldsymbol{\beta} \in \mathbb{R}^p, \boldsymbol{\gamma} \in \mathbb{R}^{p_0}} \left\{ \frac{1}{2N} \|\mathbf{Y} - \mathbf{X}\boldsymbol{\beta} - \mathbf{B}\boldsymbol{\gamma}\|_2^2 + \lambda_1 \|\boldsymbol{\beta}\|_1 + \lambda_2 \|\boldsymbol{\gamma}\|_1 \right\}. \quad (7)$$

2.4 Theoretical properties

We first study the consistency of the proposed estimator (7) under the heterogeneous-intercept model specified in (2). All regularity conditions are listed in the supplementary materials. We impose the regularity conditions (C1)-(C4), where the most crucial one is the sparse synthetic approximation (SSA) condition (C1), which assumes that the cluster-specific intercepts can be approximated by a sparse linear combination of the columns of \mathbf{B} , with approximation error δ_m . This is analogous to the approximate sparsity assumption commonly used in high-dimensional regression and semiparametric inference (Bickel et al., 2009; Bunea et al., 2007; Belloni et al., 2014). Related assumptions also appear in work on factor-LASSO (Hansen and Liao, 2019) and proxy controls (Deaner, 2021), where latent factors or confounders are represented via high-dimensional observed proxies. Conditions (C2)-(C4) are standard assumptions in the high-dimensional literature (Bickel et al., 2009; Wainwright, 2019).

Theorem 2 *Under (C1)-(C4), when the tuning parameters λ_1 and λ_2 satisfy*

$$\lambda_1 \geq 8\sigma \sqrt{\frac{\log(p)}{N}}, \quad \lambda_2 \geq 8\sigma \sqrt{\frac{\log(p_0)}{N}}, \quad (8)$$

let $\bar{\lambda} = \max(\lambda_1, \lambda_2)$, $\boldsymbol{\theta} = (\boldsymbol{\beta}^\top, \boldsymbol{\gamma}^\top)^\top$, and $\mathbf{W} = [\mathbf{X} \ \mathbf{B}]$, we have

(I)

$$\frac{1}{N} \|\mathbf{W}(\hat{\boldsymbol{\theta}} - \boldsymbol{\theta}^0)\|_2^2 = O_p(\delta_m^2 + \bar{\lambda}^2 M);$$

(II)

$$\|\hat{\boldsymbol{\beta}} - \boldsymbol{\beta}^0\|_1 = O_p(\sqrt{M}\delta_m + \bar{\lambda}M).$$

A proof of Theorem 2 is provided in the supplementary material. Theorem 2 shows that the convergence rate of $\hat{\boldsymbol{\beta}}$ depends on δ_m , that is, how well the cluster-specific intercepts can be approximated by the cluster-level adjustment term $\mathbf{b}_i^\top \boldsymbol{\gamma}^0$. Note that these bounds are derived under the worst-case fixed- $\boldsymbol{\alpha}$ analysis, in which the approximation error is treated as an arbitrary deterministic quantity.

The next theorem shows that the SHEL estimator remains consistent without requiring the SSA condition when the α_i 's are random. In place of (C1), we impose (C5), the sparse synthetic exogeneity (SSE) condition. Under the SSE condition, model (3) can be written as

$$\mathbf{Y} = \mathbf{X}\boldsymbol{\beta}^0 + \mathbf{B}\boldsymbol{\gamma}^0 + \tilde{\boldsymbol{\epsilon}}, \quad \tilde{\boldsymbol{\epsilon}} = \mathbf{D}\mathbf{u} + \boldsymbol{\epsilon}, \quad (9)$$

where $\mathbf{u} = (u_1, \dots, u_m)^\top$ and $\tilde{\boldsymbol{\epsilon}} \perp (\mathbf{X}, \mathbf{B})$. The key implication of (C5) is that \mathbf{B} captures the dependence between $\boldsymbol{\alpha}$ and \mathbf{X} , so that the remaining error term $\tilde{\boldsymbol{\epsilon}}$ is exogenous and does not introduce structural bias.

Theorem 3 *Under (C2)-(C5), when the tuning parameters λ_1 and λ_2 satisfies (8), then*

(I)

$$\frac{1}{N} \|\mathbf{W}(\hat{\boldsymbol{\theta}} - \boldsymbol{\theta}^0)\|_2^2 = O_p(\bar{\lambda}^2 M);$$

(II)

$$\|\hat{\boldsymbol{\beta}} - \boldsymbol{\beta}^0\|_1 = O_p(\bar{\lambda}M).$$

The proof of Theorem 3 is similar to that of Theorem 1 and is therefore omitted.

3 Generalized synthetic heterogeneous-effects LASSO

3.1 The GSHEL estimator

We now consider the generalized linear heterogeneous-intercepts models. Under (1), let $\ell(\xi; y)$ denote the negative log-likelihood function for the natural parameter ξ . Using the same cluster-constant matrix \mathbf{B} defined in Section 2, we propose the following generalized SHEL (GSHEL) estimator:

$$(\hat{\boldsymbol{\beta}}, \hat{\boldsymbol{\gamma}}) = \arg \min_{\boldsymbol{\beta} \in \mathbb{R}^p, \boldsymbol{\gamma} \in \mathbb{R}^{p_0}} \left\{ \frac{1}{N} \sum_{i,j} \ell(\mathbf{X}_{ij}^\top \boldsymbol{\beta} + \mathbf{b}_i^\top \boldsymbol{\gamma}; y_{ij}) + \lambda_1 \|\boldsymbol{\beta}\|_1 + \lambda_2 \|\boldsymbol{\gamma}\|_1 \right\}. \quad (10)$$

3.2 Theoretical properties

Let P_δ denote the joint probability law of (Y, W) for a given distribution of the residual effects \mathbf{u} defined in (C1), indexed by its size $\delta = \delta_m$. Let $\boldsymbol{\theta} = (\boldsymbol{\beta}^\top, \boldsymbol{\gamma}^\top)^\top$ and denote $\mathcal{L}_\delta(\boldsymbol{\theta}) = E_\delta[\ell(W^\top \boldsymbol{\theta}; Y)]$ to be the population risk, with the corresponding *marginal model parameter* defined as

$$\tilde{\boldsymbol{\theta}}_\delta = \arg \min_{\boldsymbol{\theta} \in \mathbb{R}^{p+p_0}} \mathcal{L}_\delta(\boldsymbol{\theta}). \quad (11)$$

Equivalently, $\tilde{\boldsymbol{\theta}}_\delta$ solves the population score equation $E_\delta[\nabla \ell(W^\top \boldsymbol{\theta}; Y_{ij})] = 0$. Unlike the marginal linear model (4), ignoring the heterogeneous intercepts in a GLM does not only

add extra noise, but also changes the population score equation and hence the estimation target itself. Therefore, $\tilde{\boldsymbol{\theta}}_\delta$ should be interpreted as the pseudo-true parameter under the misspecified marginal model induced by residual cluster heterogeneity of size δ .

We impose regularity conditions (G1)-(G3) on the log-likelihood function. Condition (G1) imposes a local strong convexity condition on the natural parameter scale. Condition (G2) requires the score vector $\nabla\mathcal{L}_N(\tilde{\boldsymbol{\theta}}_\delta)$ to have sub-Gaussian tail behavior, which commonly follows from the Bernstein-type inequalities under standard moment and boundedness conditions for canonical GLM (Van de Geer, 2019; Negahban et al., 2009). Both conditions are standard in the analysis of high-dimensional GLM estimators (Negahban et al., 2009). Condition (G3) requires local regularity of the population Hessian around the true parameter value.

Theorem 4 *Under (C2)-(C4) and (G1)-(G2), when the tuning parameters λ_1 and λ_2 satisfies*

$$\lambda_1 \geq A\sqrt{\frac{\log(p)}{N}}, \quad \lambda_2 \geq A\sqrt{\frac{\log(p_0)}{N}}, \quad (12)$$

where A satisfies $A > \sqrt{2/c}$ and c is the positive constant defined in (G2), then:

$$\|\hat{\boldsymbol{\beta}} - \tilde{\boldsymbol{\beta}}_\delta\|_1 = O_p(\bar{\lambda}\tilde{M}),$$

where $\tilde{M} = |\tilde{\mathcal{M}}|$ and $\tilde{\mathcal{M}} = \text{supp}(\tilde{\boldsymbol{\theta}}_\delta)$.

Theorem 4 is a direct extension of the standard consistency result for the GLM LASSO, with $\tilde{\boldsymbol{\beta}}_\delta$ playing the role of the target parameter under the misspecified marginal model. A proof is provided in the supplementary material.

Theorem 5 Under (C1) and (G3), there exists $\delta_0 > 0$ such that for all $|\delta| \leq \delta_0$,

$$\|\tilde{\beta}_\delta - \beta^0\|_2 = O(\delta).$$

Theorem 5 establishes the continuity of $\tilde{\beta}_\delta$ at $\delta = 0$. In particular, it implies that $\tilde{\beta}_\delta \rightarrow \beta^0$ as $\delta \rightarrow 0$. A proof is provided in the supplementary material.

A sufficient condition for $\tilde{\beta}_\delta$ to preserve the sparsity pattern of β^0 is that marginalizing over the residual cluster effect does not change the index direction of the model. Specifically, suppose that, conditional on the residual cluster effect u_i , the model takes the form

$$E(Y_{ij} | \mathbf{X}_{ij}, u_i) = b'(\mathbf{X}_{ij}^\top \beta^0 + u_i),$$

where $u_i \perp\!\!\!\perp \mathbf{X}_{ij}$ and $b'(\cdot)$ is the mean function associated with the exponential family. If there exists a scalar $c_\delta > 0$ such that $E_u \{b'(\eta + u_i)\} \approx b'(c_\delta \eta)$, for η in a neighborhood of the relevant linear predictors, then the marginal mean approximately preserves the same index direction. In that case, the corresponding marginal-model parameter satisfies $\tilde{\beta}_\delta \approx c_\delta \beta^0$, so that $\tilde{\beta}_\delta$ approximately preserves the support of β^0 . For an example of the logistic regression with $u_i \sim N(0, \delta^2)$, using the cumulative Gaussian approximation to the logistic function (Zeger et al., 1988), we obtain $\tilde{\beta}_{\delta,l} \approx \frac{\beta_l^0}{\sqrt{1+c^2\delta^2}}$, where $c = \frac{16\sqrt{3}}{15\pi}$.

4 Post-selection inference

4.1 Selective inference for SHEL

Although Theorem 2 and 3 prove the consistency of the proposed estimator, making valid inferences on the selected variables, even asymptotically, remains a challenging task, partially due to the lack of oracle properties of LASSO-type estimators (Fan and Li, 2001).

The selective inference approach developed by Lee et al. (2016) provides a valid framework to make inferences on variables selected by LASSO in linear fixed-effects models. Since we have a fixed-effects approach, we can adapt this framework to the SHEL estimator. To rewrite (7) as a standard LASSO problem, define

$$\mathbf{Z} = \mathbf{W} \text{diag}(\mathbf{w}^{-1}), \quad \boldsymbol{\phi} = \text{diag}(\mathbf{w})\boldsymbol{\theta},$$

where $\mathbf{w} = (w_1, \dots, w_{p+p_0})^\top$ is the penalty-weight vector. Then (7) can be expressed as:

$$\hat{\boldsymbol{\phi}} = \arg \min_{\boldsymbol{\phi} \in \mathbb{R}^{p+p_0}} \left\{ \frac{1}{2N} \|\mathbf{Y} - \mathbf{Z}\boldsymbol{\phi}\|_2^2 + \lambda_1 \|\boldsymbol{\phi}\|_1 \right\}.$$

Let $\hat{\mathcal{M}} = \text{supp}(\hat{\boldsymbol{\phi}})$ denote the active set, and let $\hat{\mathbf{s}}$ denote the corresponding sign vector. By the Karush-Kuhn-Tucker (KKT) conditions, for any fixed active set \mathcal{M} and sign vector \mathbf{s} , the selection event can be represented as a polyhedron in the data space:

$$\{\hat{\mathcal{M}} = \mathcal{M}, \hat{\mathbf{s}}_{\mathcal{M}} = \mathbf{s}\} = \{\mathbf{A}(\mathcal{M}, \mathbf{s})\mathbf{Y} \leq \mathbf{b}(\mathcal{M}, \mathbf{s})\}. \quad (13)$$

The explicit forms of $\mathbf{A}(\mathcal{M}, \mathbf{s})$ and $\mathbf{b}(\mathcal{M}, \mathbf{s})$ are provided in the supplementary material.

For any contrast vector $\boldsymbol{\eta} \in \mathbb{R}^N$, conditioning on the selection event is therefore equivalent to conditioning on the polyhedron $\{\mathbf{A}\mathbf{Y} \leq \mathbf{b}\}$. Let $TN(\mu, \sigma^2, a, b)$ denote the $N(\mu, \sigma^2)$ distribution truncated to $[a, b]$, with cumulative distribution function

$$T_{\mu, \sigma^2}^{[a, b]}(x) = \frac{\Phi\left(\frac{x-\mu}{\sigma}\right) - \Phi\left(\frac{a-\mu}{\sigma}\right)}{\Phi\left(\frac{b-\mu}{\sigma}\right) - \Phi\left(\frac{a-\mu}{\sigma}\right)}. \quad (14)$$

Under the Gaussian model $\mathbf{Y} \sim N(\boldsymbol{\mu}, \boldsymbol{\Sigma})$, Lee et al. (2016) showed that

$$[\boldsymbol{\eta}^\top \mathbf{Y} \mid \{\mathbf{A}\mathbf{Y} \leq \mathbf{b}\}] \sim TN(\boldsymbol{\eta}^\top \boldsymbol{\mu}, \boldsymbol{\eta}^\top \boldsymbol{\Sigma} \boldsymbol{\eta}, L, U),$$

where the truncation limits L and U are given in the supplementary material.

We consider two settings for applying this framework to the SHEL estimator. First, under the SSA condition (C1), when the synthetic-approximation error is negligible, model (3) is well approximated by $\mathbf{Y} = \mathbf{W}\boldsymbol{\theta}^0 + \boldsymbol{\epsilon}$. If, in addition, $\boldsymbol{\epsilon} \sim N(0, \sigma^2 \mathbf{I}_N)$, then the standard selective-inference pivot applies directly. For a selected coefficient ϕ_l , define $\boldsymbol{\eta}_l = \mathbf{Z}_{\mathcal{M}}(\mathbf{Z}_{\mathcal{M}}^\top \mathbf{Z}_{\mathcal{M}})^{-1} \mathbf{e}_l$. The pivot statistic is then $T^l = T_{\phi_l, \sigma^2 \|\boldsymbol{\eta}_l\|_2^2}^{[L, U]}(\boldsymbol{\eta}_l^\top \mathbf{Y})$. Under the null hypothesis for the selected target coefficient, we have

$$T^l \mid \{\hat{\mathcal{M}} = \mathcal{M}, \hat{\mathbf{s}}_{\mathcal{M}} = \mathbf{s}\} \sim U(0, 1).$$

Accordingly, a $(1 - \alpha)$ confidence interval for ϕ_j can be constructed by inverting the pivot.

When the SSA approximation error is small but not exactly zero, the above pivot remains approximately valid. Intuitively, the synthetic-approximation error perturbs the conditional law of $\boldsymbol{\eta}_l^\top \mathbf{Y}$ away from the ideal truncated Gaussian law by an amount controlled by δ_m . This is summarized in the following proposition.

Proposition 1 *Suppose $\boldsymbol{\epsilon} \sim N(0, \sigma^2 \mathbf{I}_N)$. For a fixed selection state $(\mathcal{M}, \mathbf{s})$, there exists a constant $C > 0$ such that*

$$\sup_{x \in [0, 1]} |P\{T^l \leq x \mid (\mathcal{M}, \mathbf{s})\} - x| \leq C \frac{\sqrt{N} \delta_m}{\sigma} + o(1).$$

The proof is provided in the supplementary material. Therefore, the standard selective-inference pivot is asymptotically valid if $\delta_m = o_p(N^{-1/2})$.

When δ_m is not negligible, exact selective inference under an i.i.d. Gaussian working model is no longer appropriate. However, under the SSE condition, if we further assume $u_i \sim N(0, \tau^2)$, then $\mathbf{Y} = \mathbf{W}\boldsymbol{\theta}^0 + \tilde{\boldsymbol{\epsilon}}$, where $\tilde{\boldsymbol{\epsilon}} \sim N(0, \boldsymbol{\Omega})$ with $\boldsymbol{\Omega} = \sigma^2 \mathbf{I}_N + \tau^2 \mathbf{D}\mathbf{D}^\top$. In this case, the response remains Gaussian, but with clustered covariance. The same polyhedral selective-inference argument therefore applies after replacing the covariance matrix in the pivot by $\boldsymbol{\Omega}$: $T^l = T_{\phi_l, \boldsymbol{\eta}_l^\top \boldsymbol{\Omega} \boldsymbol{\eta}_l}^{[L, U]}(\boldsymbol{\eta}_l^\top \mathbf{Y})$. Thus, the polyhedral selective-inference framework extends naturally to clustered Gaussian errors, given that the covariance structure is correctly incorporated.

For computational simplicity, we condition on both the active set and the sign vector throughout this article. Additional technical details are given in the supplementary material.

4.2 Debiased GSHEL

The selective inference approach introduced in Section 4.1 is constructed based on the linear selection and normality of Y in linear regression models, resulting in the exact polyhedron geometry and the exact truncated normality of the pivot statistics, which remain valid in high-dimensional settings. In a GLM, however, analogous selective-inference procedures rely on asymptotic normality of the score vector, and controlling the approximation error typically requires p to remain fixed (Taylor and Tibshirani, 2018).

For the post-selection inference of GSHEL, we instead adapt the debiased LASSO approach (Zhang and Zhang, 2014; Van de Geer et al., 2014). Let $\boldsymbol{\Sigma}_\delta = \mathbb{E}_\delta \left\{ \nabla^2 \ell(\mathbf{W}^\top \tilde{\boldsymbol{\theta}}_\delta; Y) \right\}$ denote the population Hessian matrix and $\boldsymbol{\Omega}_\delta = \boldsymbol{\Sigma}_\delta^{-1}$. For a target index $l \in \{1, \dots, p\}$, let $\mathbf{a}_l^0 = \boldsymbol{\Omega}_{\delta, l}$ denote the l th column of $\boldsymbol{\Omega}_\delta$. By inverting the KKT condition, Van de Geer et al. (2014)

proposed the one-step bias-corrected estimator

$$\hat{\beta}_l^1 = \hat{\beta}_l - \hat{\mathbf{a}}_l^\top \nabla \mathcal{L}_N(\hat{\boldsymbol{\theta}}) = \hat{\beta}_l + \hat{\mathbf{a}}_l^\top \frac{1}{N} \sum_{i,j} \mathbf{W}_{ij} (y_{ij} - \hat{\mu}_{ij}), \quad (15)$$

where $\hat{\mathbf{a}}_l$ is an estimator of \mathbf{a}_l^0 . The purpose of the correction term is to remove the first-order shrinkage bias induced by the L_1 penalty.

To estimate \mathbf{a}_l^0 , one commonly assumes that $\boldsymbol{\Omega}_\delta$ is sparse and uses a nodewise regression argument (Meinshausen and Bühlmann, 2006; Van de Geer et al., 2014). Specifically, let $\tilde{\mathbf{X}} = \mathbf{V}^{1/2} \mathbf{X}$, where $\mathbf{V} = \mathbf{V}(\hat{\boldsymbol{\theta}})$ denotes the working variance matrix of \mathbf{Y} . For the target coefficient $\tilde{\beta}_{\delta,l}$, we apply the proposed GSHEL estimator in (7) with \tilde{X}_l as the response, $\tilde{\mathbf{X}}_{-l}$ as the covariates, and \mathbf{B} as the synthetic-approximation variables. Let $\hat{\boldsymbol{\zeta}}_l$ denote the resulting coefficient estimate, and define $\hat{\mathbf{a}}_l = \hat{\sigma}_l^{-2} (1, -\hat{\boldsymbol{\zeta}}_l^\top)^\top$, where $\hat{\sigma}_l^2 = \frac{1}{N} \left\| \tilde{X}_l - \tilde{\mathbf{X}}_{-l}^\top \hat{\boldsymbol{\zeta}}_l \right\|_2^2$. At the population level, the debiasing step requires $\boldsymbol{\Sigma}_\delta \mathbf{a}_l^0 = \mathbf{e}_l$, so that the score

$$\mathbf{a}_l^{0,\top} \frac{1}{N} \sum_{i,j} \mathbf{W}_{ij} (y_{ij} - \mu_{ij})$$

is orthogonal to the nuisance directions. The nodewise regression step estimates \mathbf{a}_l^0 through a sparse approximation to the linear projection of \tilde{X}_l onto the column space of $\tilde{\mathbf{X}}_{-l}$. When $\tilde{\mathbf{X}}$ is multivariate Gaussian, this linear projection is exact, and \mathbf{a}_l^0 reflects the corresponding conditional independence structure (Ye et al., 2026). For non-Gaussian $\tilde{\mathbf{X}}$, the linear projection remains well defined whenever the second moment of \tilde{X}_l exists. Under conditions analogous to those in Section 2, namely,

$$\tilde{X}_{l,ij} = \tilde{\mathbf{X}}_{-l,ij}^\top \boldsymbol{\zeta}_l^0 + \alpha_{l,i} + \epsilon_{l,ij},$$

we impose the regularity condition (C6) on $\hat{\mathbf{a}}_l$.

Because some of the \tilde{X}_l may have heterogeneous conditional means across clusters through $\alpha_{l,i}$, the SSA condition is required for the nodewise regression step in (C6), and the proposed SHEL estimator, rather than the naive LASSO, should be used to construct the synthetic approximation. We therefore consider a cluster-level central limit theorem:

Theorem 6 For any $l \in \mathcal{P}$, under (C2)-(C6) and (G1)-(G2), let

$$\phi_{l,ij} = -\mathbf{a}_l^{0,\top} \nabla l(\mathbf{W}_{ij}^\top \tilde{\boldsymbol{\theta}}_\delta; y_{ij}), \quad \Phi_{l,i} = \sum_{j=1}^{n_i} \phi_{l,ij}, \quad V_l = \lim_{m \rightarrow \infty} \frac{1}{m} \sum_{i=1}^m \text{Var}(\Phi_{l,i}).$$

Assume further that $\sup_i E(\Phi_{l,i}^4) \leq C < \infty$ for some constant C , and that $0 < V_l < \infty$. Then:

(I)

$$\sqrt{m}(\hat{\beta}_l^1 - \tilde{\beta}_{\delta,l}) = \frac{1}{\sqrt{m}} \sum_{i=1}^m \Phi_{l,i} + o_p(1);$$

(II)

$$\sqrt{m}(\hat{\beta}_l^1 - \tilde{\beta}_{\delta,l}) \xrightarrow{d} N(0, V_l);$$

(III) $\hat{V}_l \xrightarrow{P} V_l$, where

$$\hat{\phi}_{l,ij} = -\hat{\mathbf{a}}_l^\top \nabla l(\mathbf{W}_{ij}^\top \hat{\boldsymbol{\theta}}; y_{ij}), \quad \hat{\Phi}_{l,i} = \sum_{j=1}^{n_i} \hat{\phi}_{l,ij}, \quad \hat{V}_l = \frac{1}{m} \sum_{i=1}^m \hat{\Phi}_{l,i}^2.$$

Theorem 6 is stated under a cluster-level central limit theorem. This formulation is appropriate under the SSE condition, where the residual cluster heterogeneity is not asymptotically negligible, and therefore induces persistent within-cluster dependence. When δ_m is sufficiently small, however, the residual within-cluster dependence becomes negligible, and the debiased GSHEL can adapt to the standard debiased-LASSO based on observation-level asymptotic

linearity. In that case, the limiting distribution may be normalized at the usual \sqrt{N} rate, and the corresponding variance reduces to the familiar i.i.d. form.

5 Algorithm

We now address some implementation issues of the proposed estimation procedures and further propose extended iterative algorithms.

5.1 Implementation of the SHEL and GSHEL

The SHEL estimator (7) can be re-expressed as

$$\hat{\boldsymbol{\theta}} = \arg \min_{\boldsymbol{\theta} \in \mathbb{R}^{p+p_0}} \left\{ \frac{1}{2N} \|\mathbf{Y} - \mathbf{W}\boldsymbol{\theta}\|_2^2 + \lambda_1 \sum_{k=1}^{p+p_0} w_k |\theta_k| \right\}, \quad (16)$$

where $w_k = 1$ for the $\boldsymbol{\beta}$ -coordinates and $w_k = \lambda_2/\lambda_1$ for the $\boldsymbol{\gamma}$ -coordinates. Thus, SHEL can be viewed as a weighted LASSO estimator. Similarly, the GSHEL estimator (10) can be re-expressed as

$$\hat{\boldsymbol{\theta}} = \arg \min_{\boldsymbol{\theta} \in \mathbb{R}^{p+p_0}} \left\{ \frac{1}{N} \sum_{i,j} l(\mathbf{W}_{ij}^\top \boldsymbol{\theta}; y_{ij}) + \lambda_1 \sum_{k=1}^{p+p_0} w_k |\theta_k| \right\}. \quad (17)$$

As suggested in Theorems 2-4, the consistency of the proposed estimator requires $\lambda_1/\lambda_2 = O(\sqrt{\log(p)/\log(p_0)})$. To reduce the computational burden, we set $\lambda_2 = \lambda_1 \sqrt{\log(p_0)/\log(p)}$, and select λ_1 by K -fold cross-validation. To construct the cluster-constant matrix \mathbf{B} , we propose testing each covariate for between-cluster heterogeneity. For a continuous covariate X_l , we perform an ANOVA, and for a categorical covariate X_l , we fit a generalized random-intercepts model and test whether the between-cluster variance is zero. We then include in \mathbf{B} the cluster means of those covariates whose p-values are below a pre-specified significance

level. The resulting SHEL/GSHEL fit can then be used for the post-selection inference procedures in Section 4. See details in Algorithm 1 of the supplementary material.

5.2 Iterative SHEL and GSHEL

The consistency of the SHEL and GSHEL estimators relies on the sparsity condition $M = M_1 + M_2 = o\{\sqrt{N}/\log(p)\}$. This condition is often plausible when endogenous covariates are present, as is common in observational studies (Grilli and Rampichini, 2011). However, when $\mathbf{B} \perp\!\!\!\perp \boldsymbol{\alpha}$, the optimal solution $\boldsymbol{\gamma}^0$ need not be sparse, because the synthetic approximation may be driven mainly by spurious correlations between the cluster means of the covariates and $\boldsymbol{\alpha}$. More precisely, Mulayoff and Michaeli (2019) showed that $\delta_m = O_p\left(\left(p_0/m\right)^{-\frac{a}{1-a}}\right)$, where $a = M_2/m \in (0, 1)$ is the sparsity fraction. Although Theorems 3 and 4 show that $\delta_m \rightarrow 0$ is not necessary for consistency of SHEL or GSHEL, sparsity of the full parameter vector $\boldsymbol{\theta}$ is still required. Since the primary inferential target is $\boldsymbol{\beta}$, the coefficient vector $\boldsymbol{\gamma}$ may be viewed as a nuisance parameter. Motivated by this observation, we propose iterative versions of SHEL and GSHEL, denoted ISHEL and IGSHEL, in which the final fitting step in Algorithm 1 is repeated while conditioning on the estimated synthetic approximation from the previous iteration.

Let $\widehat{\mathbf{D}\boldsymbol{\alpha}}^{(s)} = \mathbf{B}\hat{\boldsymbol{\gamma}}^{(s)}$ denote the estimated synthetic approximation at iteration s . At each step, we augment the current design with $\widehat{\mathbf{D}\boldsymbol{\alpha}}^{(s-1)}$ from the previous iteration and refit the penalized model. The algorithm stops when $\left\|\widehat{\mathbf{D}\boldsymbol{\alpha}}^{(s)} - \widehat{\mathbf{D}\boldsymbol{\alpha}}^{(s-1)}\right\|_2^2 < e_{\text{thr}}$. This iterative scheme can yield a sparser final solution. However, because the design is updated in a data-dependent manner across iterations, the post-selection inference procedures developed in Section 4 do not directly apply to ISHEL or IGSHEL. See details in Algorithm 2 of the supplementary material.

6 Simulation studies

6.1 Simulation settings

We consider $m = 400$, $n = n_i = 4$ for all $i = 1, \dots, m$, and $p = 1000$ covariates. The heterogeneous intercepts α_i are randomly sampled from F_α . We generate the covariates \mathbf{X}_{ij} from a multivariate Gaussian distribution with mean vector $\boldsymbol{\mu}_i$ and precision matrix Θ . Specifically, Θ is taken to be block diagonal with block size 5. Within each block, we set $\Theta_{ll} = 1$ and $\Theta_{ll'} = 0.5$ for $l \neq l'$. For each replication, we randomly select $p_0 = 0, 50, 100, 200, 500$, or 800 covariates to have heterogeneous distributions across clusters. That is, for $l \in \mathcal{P}_0^c$, we set $\mu_{l,i} = 0$ for all i ; for $l \in \mathcal{P}_0$, the cluster-specific means $\mu_{l,i}$ are independently sampled from F_l .

We consider two specifications for F_α and F_l . The first, denoted by ‘‘Independent’’, assumes that F_α and F_l are independent for all l . In this setting, we let each F_l be a standard Gaussian distribution, and let F_α follow either a standard Gaussian distribution or a Gaussian mixture, $(0.5N(-1, 0.5) + 0.5N(1, 0.5))$. In the second setting, denoted by ‘‘Endogenous’’, we first generate a latent variable U_i , and then generate $\mu_{l,i}$ and α_i according to

$$\mu_{l,i} = h_l U_i + n^{-1} Z_{l,i}, \quad \alpha_i = 0.8 U_i + 0.2 Z_i,$$

where $Z_{l,i}$ and Z_i follow standard Gaussian distributions and $h_l \sim U(0, 1)$. As in the Independent setting, we let U_i follow either a standard Gaussian or a Gaussian mixture.

We consider both the LMM in (2) and the GLMM in (1) with a logistic link function. We set $\mathcal{M}_1 = \{1, 6, 11, 12, 16, 17\}$ and $\boldsymbol{\beta}_{\mathcal{M}_1} = (0.5, 0.5, 1, 1, 1.5, 1.5)^\top$. To evaluate variable selection performance, we record the number of false positives (FP) and true positives (TP). For the LMM, parameter estimation and prediction performance are assessed using the root mean squared error (RMSE), $\|\hat{\boldsymbol{\beta}} - \boldsymbol{\beta}^0\|_1$, and the residual ICC. For the GLMM, prediction

performance is evaluated using sensitivity and specificity. For post-selection inference, we report the false positive rate (FPR), power, and median length of the 95% confidence interval (median CI length). The definitions of these measures are given in Table S1. All performance measures are computed from 200 simulated datasets.

For variable selection, parameter estimation, and prediction, we compare the proposed SHEL/GSHEL and ISHEL/IGSHEL algorithms with the marginal model LASSO estimator. For all methods, the tuning parameter is selected by ten-fold cross-validation (CV). Specifically, we choose λ either by minimizing the CV error (λ_{\min}) or by using the one-standard-error rule (λ_{1se}) (Hastie et al., 2009). In the iterative procedure, “ISHEL1” uses $\lambda_1 = \lambda_{1se}$ in Step 6 of Algorithm 2, whereas “ISHEL2” uses $\lambda_1 = \lambda_{\min}$. For post-selection inference, we consider the exact polyhedral selective inference (SI) method introduced in Section 4.1 and the debiased SHEL method introduced in Section 4.2 for variables selected by SHEL in LMMs. SI1 refers to the T_l calculated ignoring the within-cluster correlation, motivated by Lemma 1; SI2 refers to the T_l calculated with $\hat{\Omega} = \hat{\sigma}^2 \mathbf{I}_N + \hat{\tau}^2 \mathbf{D}\mathbf{D}^\top$, where $\hat{\sigma}^2$ and $\hat{\tau}^2$ are obtained by fitting a random intercepts model on the model residual. For variables selected by GSHEL in GLMM, only the debiased GSHEL method is considered. As a benchmark, we also include a naive analysis that refits the selected variables using the corresponding LMM or GLMM via unpenalized maximum likelihood estimation.

6.2 Simulation results for variable selection, parameter estimation, and prediction

Across all settings, all methods are able to identify all nonzero coefficients, yielding TP = 6. For LMM with Gaussian random effects, the numbers of false positives, RMSE, $\|\hat{\boldsymbol{\beta}} - \boldsymbol{\beta}^0\|_1$, and residual ICC are presented in Figures 1 and 2. As expected, λ_{1se} generally leads to better variable selection performance, whereas λ_{\min} tends to yield better prediction

performance.

When $p_0 = 0$, as suggested in Theorem 1, no covariates are available to synthesize the random intercepts, and the marginal model LASSO estimator is equivalent to our proposed method, which, on the one hand, consistently estimates the targeted parameter β^0 , as reflected by the small values of $\|\hat{\beta} - \beta^0\|_1$ and FP, but on the other hand, results in relatively larger RMSE and residual ICC compared to cases with $p_0 > 0$, as the omitted random intercepts are absorbed into the residual variation.

As p_0 increases, the marginal model LASSO estimator tends to include more noise variables, resulting in larger FP and estimation error $\|\hat{\beta} - \beta^0\|_1$. This degradation is due to contamination from γ^* , as suggested in Theorem 1. Comparing the two dependence settings, the marginal-model LASSO is less sensitive to increases in p_0 under the Independent setting than under the Endogenous setting. This is because, under the Independent setting, the synthetic approximation is driven mainly by high-dimensional spurious correlations among variables in \mathcal{P}_0 , rather than by genuine dependence between the covariates and the random intercepts. In contrast, our proposed method performs similarly to the benchmark case with $p_0 = 0$.

For both the proposed methods and the marginal-model LASSO, RMSE and residual ICC decrease as p_0 increases, reflecting the increasing ability of the synthetic approximation to explain cluster-level heterogeneity. Comparing SHEL and ISHEL, the two methods perform similarly under the Endogenous setting, whereas ISHEL outperforms SHEL under the Independent setting. This is consistent with the discussion in Section 5.2: under Independence, the optimal coefficient vector γ^0 is generally not sparse because the synthetic approximation relies on accumulated spurious high-dimensional correlations, and the iterative procedure is better suited to accommodate this structure.

For GLMM with Gaussian random effects, the numbers of false positives, sensitivity, and

specificity are presented in Figures S1 and S2. Overall, the conclusions are similar to those for the LMM. However, in the GLMM setting, the marginal-model LASSO appears to be less affected by contamination from γ^* . In addition, the proposed methods show similar performance under Gaussian mixture random effects (see Figures S3-S6), suggesting that they are robust to deviations from Gaussianity in the random effects distribution.

6.3 Simulation results for post-selection inference

Results for LMM with Gaussian random effects are summarized in Figure 3. The naive analysis substantially inflates the FPR in all settings. Under the Independent setting, both SI2 and debiased SHEL control the FPR at the nominal level on average, whereas SI slightly inflates the type I error rate when $p_0 \geq 100$. Under the Endogenous setting, debiased SHEL continues to control the FPR at the nominal level, but both SI methods inflate the type I error rate whenever $p_0 > 0$, with the degree of inflation decreasing as p_0 increases. Debiased SHEL is conservative, yielding FPRs close to 0 in all settings. In contrast, the SI methods exhibit substantially greater variability, with a noticeably larger proportion of outliers than debiased SHEL. Similar patterns are observed for power and median confidence interval length. Overall, these results suggest that the SI procedures have desirable average performance, but may be unstable in individual analyses.

Results for GLMM with Gaussian random effects are summarized in Figure S7. The overall conclusions are similar to those for the LMM. Debiased GSHEL conservatively controls the FPR, whereas the naive analysis substantially inflates it. In the Endogenous setting, although the FPR remains inflated for naive analysis in all cases, it decreases as p_0 increases. This phenomenon is only observed for the GLMM but not for the LMM. Because debiased GSHEL is conservative, it also yields lower power and longer median confidence interval length than the naive analysis. As in Section 6.2, similar performance is observed under

Gaussian mixture random effects; see Figures S8 and S9.

7 Real data analysis: longitudinal neutrophil transcriptomics in COVID-19

7.1 Background and data description

To evaluate the practical performance of the proposed GSHEL method, we applied it to a publicly available longitudinal bulk RNA-seq dataset of enriched blood neutrophils from hospitalized COVID-19 patients (LaSalle et al., 2022). The original study enrolled 306 COVID-19-positive patients at the Massachusetts General Hospital between March and May 2020. Blood samples were collected at up to three time points, including day 0 (admission), day 3, and day 7, and neutrophils were enriched from whole blood for bulk RNA sequencing. After quality control, we retained 629 samples from 306 patients. Gene expression was quantified as $\log_2(\text{TPM} + 1)$, where TPM (transcripts per million) is a normalized measure of gene expression abundance. The binary outcome was the maximum disease severity within 28 days. Age and BMI were included as candidate covariates. Data are publicly available through GEO (GSE212041).

The original study employed a multi-step pipeline: separate differential expression analyses at each time point, unsupervised non-negative matrix factorization (NMF) to identify six neutrophil subtypes, and a LASSO model using NMF metagene scores and clinical variables built on day 0 data alone. In our work, GSHEL performs variable selection in a single step, jointly leveraging all time points within the GLMM (1).

7.2 Variable selection results

Starting from 5,000 candidate genes, our screening procedure retained 3,481 genes (two-sample t -test $p < 0.05$), of which 2,397 exhibited significant within-cluster correlation (likelihood ratio test $p < 0.05$). The marginal model LASSO selected 75 genes, while GSHEL selected 37 genes, with the iterative GSHEL yielding 35 of the same 37. Neither age nor BMI was selected. The over-selection of the naive LASSO confirms the target distortion phenomenon in Theorem 1. The debiased LASSO identified 10 of the 37 genes as individually significant ($p < 0.05$). The selected genes are summarized in Table S2.

7.3 Biological interpretation

We assessed biological relevance by comparing the 37 GSHEL-selected genes with findings from the original study. Most notably, three genes, *S100A12*, *CD177*, and *MCEMP1*, are the defining markers of the granulocytic myeloid-derived suppressor cell (G-MDSC) subtype identified via NMF clustering in the original study. This subtype was the single strongest predictor of COVID-19 severity detected in LaSalle et al. (2022), with the highest NMF5 score quintile selected across all cross-validation folds. The independent recovery of these three markers by GSHEL provides strong validation of the method. Additionally, *SERPINB2*, a gene specifically highlighted in the original study for its diverging longitudinal trajectory between severe and non-severe patients, was selected, demonstrating GSHEL’s ability to capture time-varying signals directly from the main selection procedure.

Beyond these core findings, the remaining selected genes are also biologically coherent: they include MHC class II genes (*HLA-DMA*, *HLA-DMB*) associated with non-severe disease in the original study, interferon-stimulated genes (*RARRES3*, *IRF2BP2*) consistent with the reported IFN pathway enrichment, metabolic genes (*NQO2*, *ALDH1A1*) aligned with the ROS and metabolic signatures of severe disease, and known regulators of myeloid differentiation

(*HOTAIRM1*, *PDE4D*). Two immunoglobulin genes (*IGHM*, *IGLVI-70*) were also selected. LaSalle et al. (2022) noted that immunoglobulin gene expression in neutrophil-enriched samples may reflect cell-type contamination rather than true biological signal. To investigate whether the selection of the two immunoglobulin genes was driven by such contamination, a sensitivity analysis including the immunoglobulin score from the original study as a forced covariate was conducted. The sensitivity model selected 32 genes, retaining all core severity markers as well as both immunoglobulin genes, suggesting that their inclusion is not solely driven by contamination and may reflect associations with humoral immune responses and disease severity.

Among the 37 selected genes, the debiased LASSO identified 10 as individually significant ($p < 0.05$), including the two most prominently validated severity markers, *S100A12* and *SERPINB2*, as well as several other biologically supported genes, such as the interferon-stimulated gene *RARRES3*. A complete categorization is provided in Table S2.

8 Discussion

In this article, we propose the synthetic heterogeneous-effects LASSO, a framework that uses high-dimensional cluster-level covariates as synthetic approximations for latent random intercepts in high-dimensional mixed-effects models. The proposed approach is computationally feasible while retaining interpretability for the target regression coefficients. We establish consistency of the proposed estimators in both high-dimensional LMM and GLMM. We develop valid post-selection inference procedures based on both the polyhedral selective inference and the debiased LASSO.

Cluster-constant covariates. Our proposed method uses cluster means of heterogeneously distributed X_i 's to synthesize the latent random intercepts. A key feature of the framework is

that it separates the role of the covariates in parameter estimation from their role in synthetic control construction, which helps reduce the selection bias present in the marginal-model LASSO. However, this separation is no longer possible for cluster-constant covariates, because such variables enter both components in the same way.

Penalty functions. In this article, we focus on the ℓ_1 -penalty function (LASSO). Our method can be adapted to other penalty functions, such as the elastic net or SCAD, with similar theoretical properties as provided in Sections 2 and 3 held. Although debiased inference is most commonly developed for the LASSO, the underlying bias-correction idea is more general and can be extended to other penalized estimators. However, additional technical arguments are typically needed to account for their distinct shrinkage and optimization properties. For example, the main modification for the elastic net is that the KKT conditions contains an additional ridge term. Consequently, both the bias-correction step and the inverse-Hessian approximation must be constructed for the ridge-adjusted score map, and additional rate conditions are needed to ensure that the resulting bias is asymptotically negligible for inference (Zhang and Jia, 2022).

Post-selection inference for ISHEL. For the SHEL estimator, once \mathbf{B} is constructed, the design matrix entering the penalized optimization is fixed. This makes the post-selection problem comparatively tractable, since the KKT conditions lead to a well-defined geometric characterization of the selection event and the associated bias-correction arguments can be developed under a stable design. In contrast, the ISHEL algorithm repeatedly updates the synthetic approximation in a data-dependent manner, so the effective design matrix evolves with the response across iterations. Consequently, the final selection event is determined by a sequence of adaptive design updates rather than a single fixed optimization problem, and standard post-selection inference tools no longer apply directly. This iterative dependence creates substantial technical challenges for both selective-inference and debiasing-based

procedures, and developing valid inference methods for such design-updating algorithms remains an important direction for future work.

Multiple random effects. We consider only heterogeneous intercepts in this work. Other forms of cluster-level heterogeneity, such as random slopes or nested random effects, can also be synthesized by including appropriate cluster-level summary statistics in the \mathbf{B} matrix. In future work, we aspire to extend the proposed framework to accommodate multiple random effects simultaneously and to develop methods for random-effects selection.

Supplemental Material

In the supplemental material, we provide proofs of theorems, additional simulation results referenced in Section 6, and additional results referenced in Section 7.

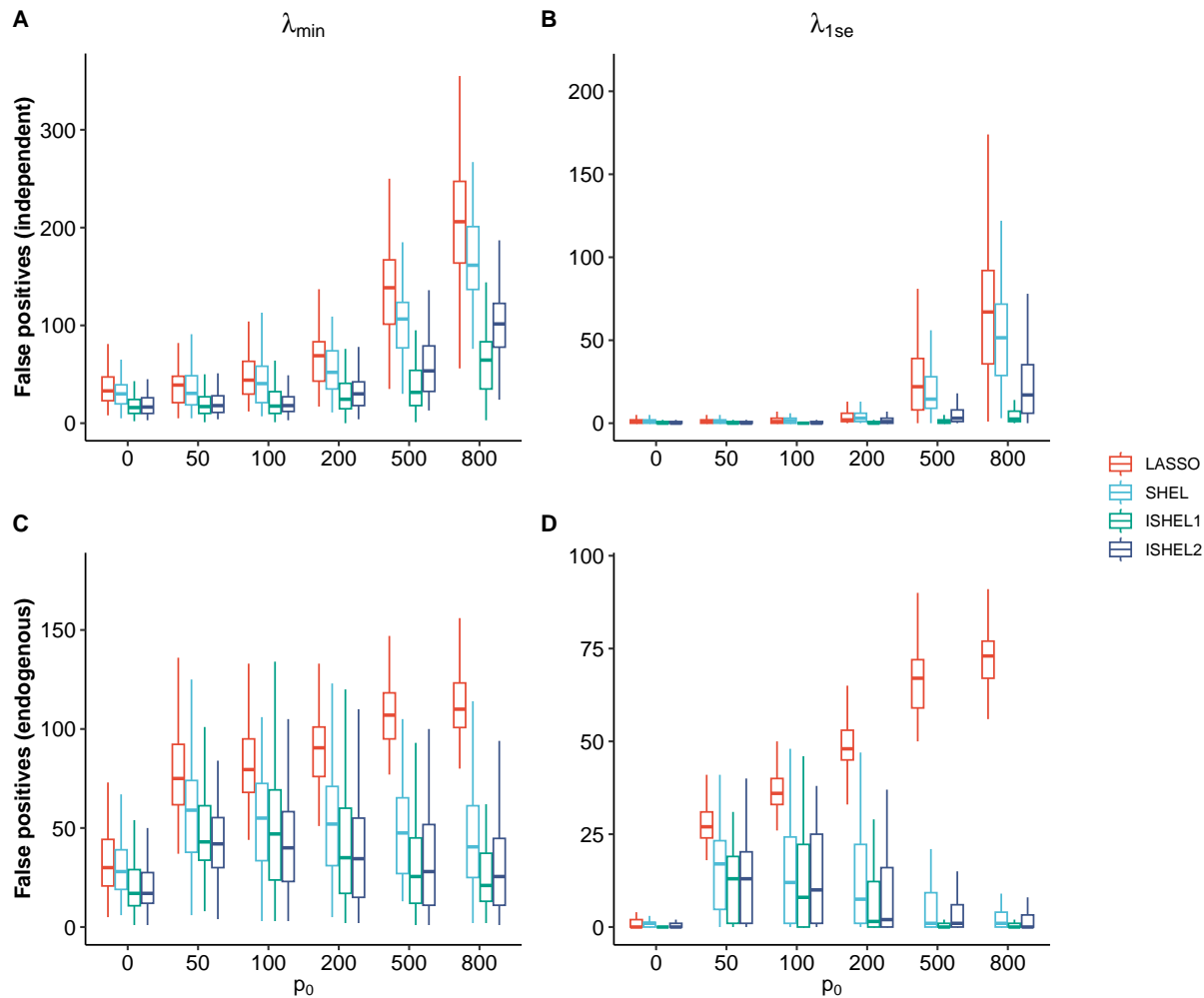


Figure 1: Number of false selections for high-dimensional linear random-effects models with Gaussian random intercepts.

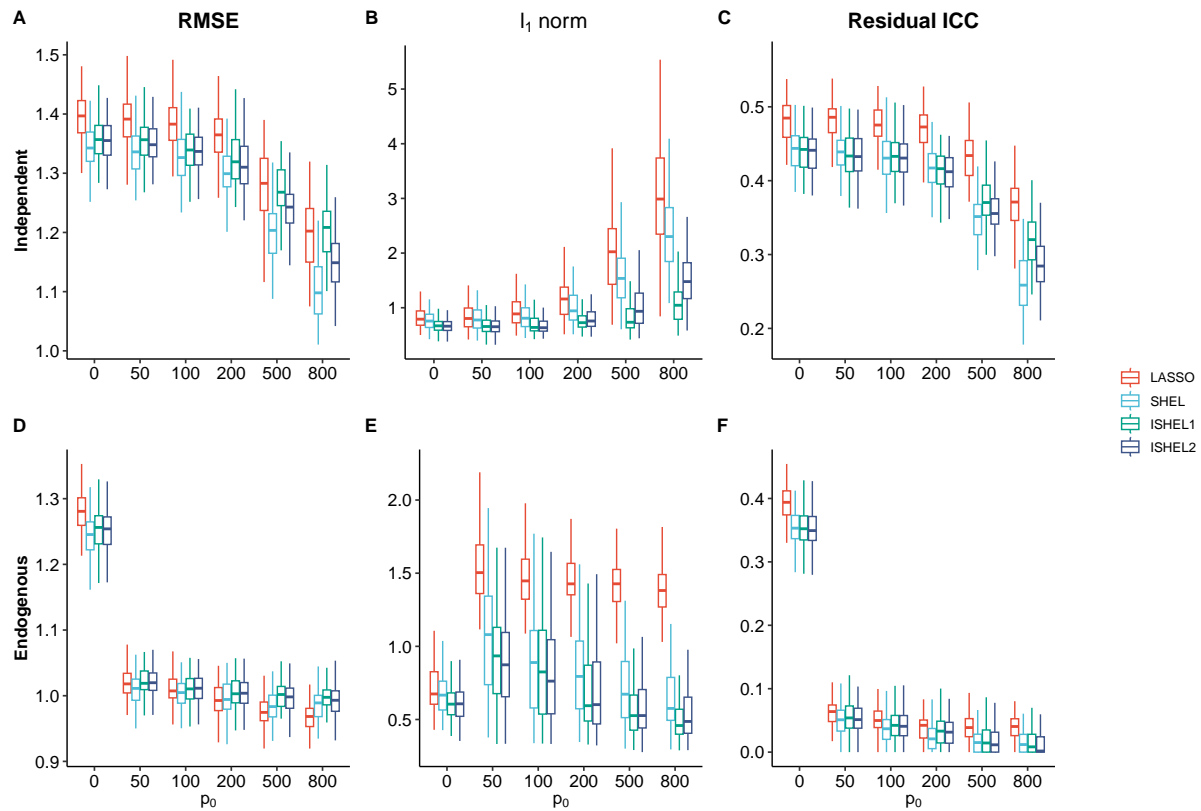


Figure 2: Empirical RMSE, $\|\hat{\beta} - \beta^0\|_1$, and residual ICC in high-dimensional linear random-intercepts models with Gaussian random intercepts.

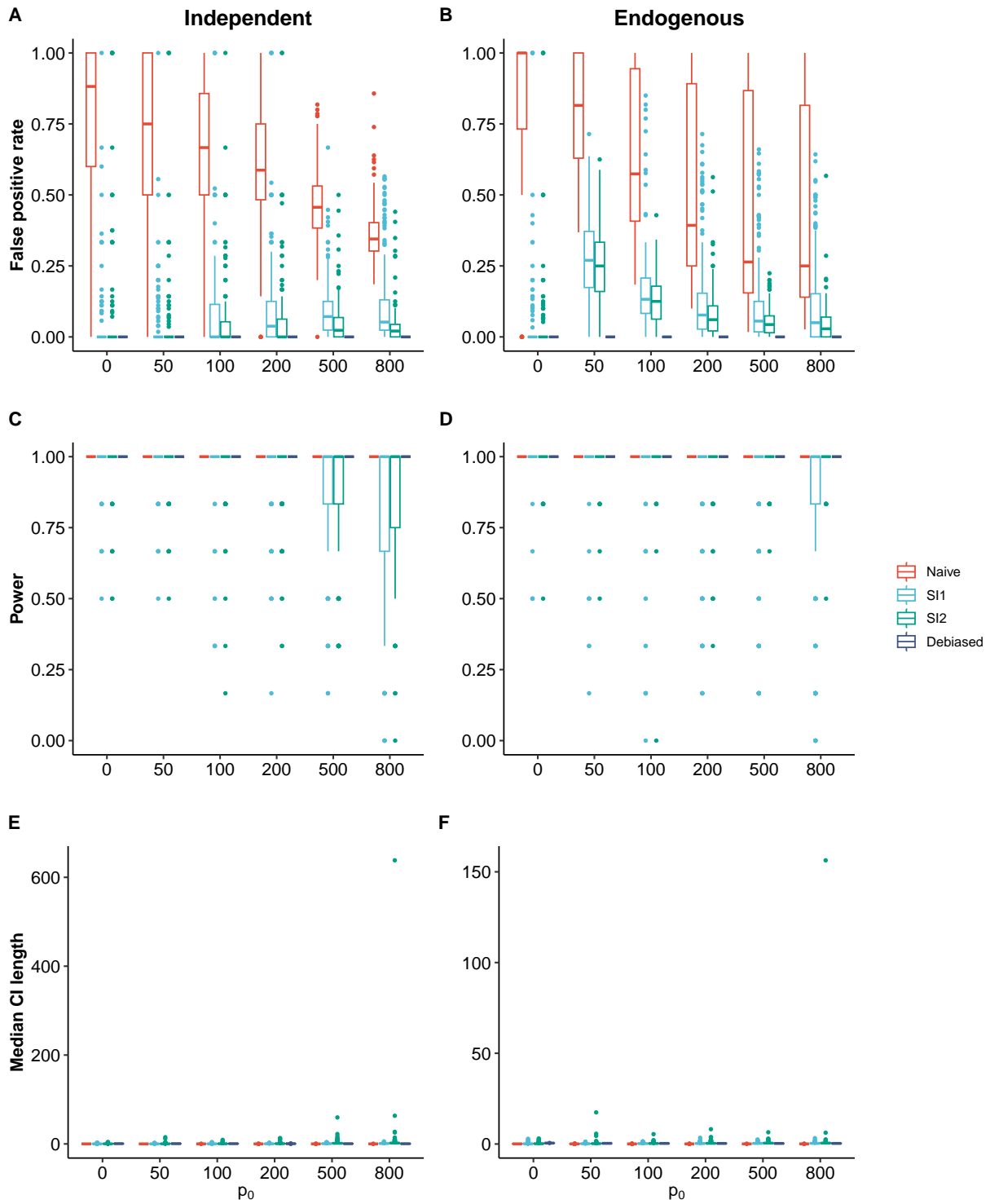


Figure 3: False positive rate, power, and median 95% CI length for Gaussian random intercepts, with variables selected from SHEL.

Supplementary Material

A Regularity conditions

(C1) Sparse synthetic approximation (SSA) condition: For the sparsity level $M_2 \in \{1, \dots, p_0\}$, there exists $\boldsymbol{\gamma}^0 \in \mathbb{R}^{p_0}$ with $\|\boldsymbol{\gamma}^0\|_0 \leq M_2$ such that

$$\alpha_i = \mathbf{b}_i^\top \boldsymbol{\gamma}^0 + u_i, \quad i = 1, \dots, m, \quad (\text{S1})$$

the $\delta_m^2 := \delta_m^2(M_2) = \frac{1}{m} \|\mathbf{u}\|_2^2$ satisfies

$$\frac{\delta_m}{\lambda_1} \rightarrow 0 \text{ as } N \rightarrow \infty,$$

where $\mathbf{u} = (u_1, \dots, u_m)^\top$.

(C2) There exist positive constants c_l and c_u such that $c_l \leq \pi_i \leq c_u$ for every $i = 1, \dots, m$, where $\pi_i = n_i/N$.

(C3) Columns of \mathbf{X} and \mathbf{B} , denoted as \mathbf{X}_l and \mathbf{B}_l , respectively, are normalized:

$$\frac{1}{N} \|\mathbf{X}_l\|_2^2 \leq 1, \quad \frac{1}{N} \|\mathbf{B}_l\|_2^2 \leq 1.$$

(C4) Restricted eigenvalue (RE) condition: Let $\mathbf{W} = [\mathbf{X} \ \mathbf{B}] \in \mathbb{R}^{N \times (p+p_0)}$, $\boldsymbol{\theta} = (\boldsymbol{\beta}^\top, \boldsymbol{\gamma}^\top)^\top$, and $\mathcal{M} = \text{supp}(\boldsymbol{\theta}^0)$ with $|\mathcal{M}| \leq M = M_1 + M_2$. Denote $\mathcal{C}_a(\mathcal{M}) \subseteq \mathbb{R}^{p+p_0}$ be a set defined as $\mathcal{C}_a(\mathcal{M}) = \{\mathbf{b} \in \mathbb{R}^{p+p_0} : \|\mathbf{b}(\mathcal{M}^c)\|_1 \leq a \|\mathbf{b}(\mathcal{M})\|_1\}$, where $a > 0$. Then \mathbf{W} satisfies the restricted eigenvalue condition for $\kappa > 0$ if $N^{-1} \|\mathbf{W}\mathbf{b}\|_2^2 \geq \kappa \|\mathbf{b}\|_2^2$, for every $\mathbf{b} \in \mathcal{C}_a(\mathcal{M})$.

(C5) Sparse synthetic exogeneity (SSE) condition: For the sparsity level $M_2 \in \{1, \dots, p_0\}$, there exists $\boldsymbol{\gamma}^0 \in \mathbb{R}^{p_0}$ with $\|\boldsymbol{\gamma}^0\|_0 \leq M_2$ such that u_i defined in (S1) are i.i.d. sub-Gaussian random variables with $E(u_i) = 0$, $E(u_i^2) = \tau^2$, and $u_i \perp\!\!\!\perp (\mathbf{X}, \mathbf{B})$.

(C6) $\|\hat{\mathbf{a}}_l - \mathbf{a}_l^0\|_1 = o_p(1)$, $\|\hat{\mathbf{a}}_l\|_1 = O_p(1)$, and

$$\left\| \nabla^2 \mathcal{L}_N(\tilde{\boldsymbol{\theta}}_\delta)(\hat{\mathbf{a}}_l - \mathbf{a}_l^0) \right\|_\infty = o_p(1).$$

(G1) $\ell(\cdot, y)$ is convex around ξ^0 and there exist positive constants C_l and C_u such that $C_l < \ell''(\xi, y) < C_u$.

(G2) Let

$$\mathcal{L}_N(\boldsymbol{\theta}) = \frac{1}{N} \sum_{i,j} \ell(\mathbf{W}_{ij}^\top \boldsymbol{\theta}; y_{ij}),$$

denote the empirical risk, where $\mathbf{W}_{ij} = (\mathbf{X}_{ij}^\top, \mathbf{b}_i^\top)^\top$. Then the gradient $\nabla \mathcal{L}_N(\tilde{\boldsymbol{\theta}}_\delta)$ satisfies

$$P\left(\|\nabla \mathcal{L}_N(\tilde{\boldsymbol{\theta}}_\delta)\|_\infty \geq t\right) \leq 2 \exp(-cNt^2)$$

for some $c > 0$.

(G3) For all δ , $\nabla^2 \mathcal{L}_\delta(\boldsymbol{\theta}^0)$ is nonsingular and Lipschitz continuous in a neighborhood of $\boldsymbol{\theta}^0$.

B Proofs

B.1 Proof of Theorem 1

Since $\boldsymbol{\beta}^* = \boldsymbol{\beta}^0 + \tilde{\boldsymbol{\gamma}}^*$, we have

$$\mathbf{Y} = \mathbf{X}\boldsymbol{\beta}^* + (\mathbf{D}\boldsymbol{\alpha} - \mathbf{X}\tilde{\boldsymbol{\gamma}}^*) + \boldsymbol{\epsilon} = \mathbf{X}\boldsymbol{\beta}^* + \mathbf{r}^* + \mathbf{e},$$

where $\mathbf{r}^* = (r_{11}^*, \dots, r_{mn_m}^*)^\top$, $\mathbf{e} = (e_{11}, \dots, e_{mn_m})^\top$, and $r_{ij}^* = \alpha_i - \boldsymbol{\mu}_{\mathcal{P}_{0,ij}}^\top \boldsymbol{\gamma}^*$. Because

$$\frac{1}{2N} \|\mathbf{Y} - \mathbf{X}\hat{\boldsymbol{\beta}}\|_2^2 + \lambda \|\hat{\boldsymbol{\beta}}\|_1 \leq \frac{1}{2N} \|\mathbf{Y} - \mathbf{X}\boldsymbol{\beta}^*\|_2^2 + \lambda \|\boldsymbol{\beta}^0\|_1,$$

we have the basic inequality:

$$\frac{1}{2N} \|\mathbf{X}\boldsymbol{\Delta}^*\|_2^2 \leq \frac{1}{N} (\mathbf{r}^* + \mathbf{e})^\top \mathbf{X}\boldsymbol{\Delta}^* + \lambda (\|\boldsymbol{\beta}^*\|_1 - \|\hat{\boldsymbol{\beta}}\|_1), \quad (\text{S2})$$

where $\boldsymbol{\Delta}^* = \hat{\boldsymbol{\beta}} - \boldsymbol{\beta}^*$. By the Holder's inequality, we have

$$\frac{2}{N} \mathbf{r}^{*,\top} \mathbf{X}\boldsymbol{\Delta}^* \leq \left\| \frac{2}{N} \mathbf{r}^{*,\top} \mathbf{X} \right\|_\infty \|\boldsymbol{\Delta}^*\|_1 \leq C\delta_m \|\boldsymbol{\Delta}^*\|_1, \quad (\text{S3})$$

where $C = 2\sqrt{c_u}$. Let \mathcal{E}^* be the set of events defined as

$$\mathcal{E}^* = \left\{ \lambda \geq \frac{2}{N} \|\mathbf{X}^\top \mathbf{e}\|_\infty \right\},$$

(S2) and (S3) implies that, under \mathcal{E}^* , we have

$$\begin{aligned} \frac{1}{N} \|\mathbf{X}\boldsymbol{\Delta}^*\|_2^2 &\leq \frac{2}{N} \mathbf{r}^{*,\top} \mathbf{X}\boldsymbol{\Delta}^* + \frac{2}{N} \|\mathbf{e}^\top \mathbf{X}\|_\infty \|\boldsymbol{\Delta}^*\|_1 + 2\lambda (\|\boldsymbol{\beta}^*\|_1 - \|\hat{\boldsymbol{\beta}}\|_1) \\ &\leq C\delta_m \|\boldsymbol{\Delta}^*\|_1 + \lambda \|\boldsymbol{\Delta}^*\|_1 + 2\lambda (\|\boldsymbol{\beta}^*\|_1 - \|\hat{\boldsymbol{\beta}}\|_1). \end{aligned} \quad (\text{S4})$$

Due to the triangle inequality, let $\mathcal{M}^* = \{\beta_i^* \neq 0\}$, we have

$$\|\boldsymbol{\beta}^*\|_1 - \|\hat{\boldsymbol{\beta}}\|_1 \leq \|\boldsymbol{\Delta}_{\mathcal{M}^*}^*\|_1 - \|\boldsymbol{\Delta}_{\mathcal{M}^{*,c}}^*\|_1. \quad (\text{S5})$$

Combining (S4) and (S5), we have

$$\begin{aligned} \frac{1}{N} \|\mathbf{X} \boldsymbol{\Delta}^*\|_2^2 &\leq C\delta_m \|\boldsymbol{\Delta}^*\|_1 + \lambda \|\boldsymbol{\Delta}^*\|_1 + 2\lambda (\|\boldsymbol{\Delta}_{\mathcal{M}^*}^*\|_1 - \|\boldsymbol{\Delta}_{\mathcal{M}^{*,c}}^*\|_1) \\ &= (3\lambda + C\delta_m) \|\boldsymbol{\Delta}_{\mathcal{M}^*}^*\|_1 - (\lambda - C\delta_m) \|\boldsymbol{\Delta}_{\mathcal{M}^{*,c}}^*\|_1. \end{aligned} \quad (\text{S6})$$

For any $e \in (0, 1)$, under (C1), we have $C\delta_m \leq \bar{\lambda}e$ holds with high probability, and

$$3\lambda + C\delta_m \leq (3 + e)\lambda, \quad \lambda - C\delta_m \geq (1 - e)\lambda,$$

which implies

$$\|\boldsymbol{\Delta}_{\mathcal{M}^{*,c}}^*\|_1 \leq \frac{3 + e}{1 - e} \|\boldsymbol{\Delta}_{\mathcal{M}^*}^*\|_1.$$

Thus, by arbitrarily choosing $e = 1/2$, we have

$$\|\boldsymbol{\Delta}_{\mathcal{M}^{*,c}}^*\|_1 \leq 7\|\boldsymbol{\Delta}_{\mathcal{M}^*}^*\|_1 \quad (\text{S7})$$

and $\boldsymbol{\Delta} \in \mathcal{C}_7(\mathcal{M}^*)$. Notice that based on Cauchy-Schwarz inequalities, we have

$$\frac{2}{N} \mathbf{r}^{*,\top} \mathbf{X} \boldsymbol{\Delta}^* \leq 4c_u \delta_m^2 + \frac{1}{4N} \|\mathbf{X} \boldsymbol{\Delta}^*\|_2^2. \quad (\text{S8})$$

Combining (S6)-(S8), we have

$$\begin{aligned}
& \frac{3}{4N} \|\mathbf{X} \Delta^*\|_2^2 + \lambda \|\Delta^*\|_1 \\
&= \frac{3}{4N} \|\mathbf{X} \Delta^*\|_2^2 + \lambda \|\Delta^*_{\mathcal{M}^*}\|_1 + \lambda \|\Delta^*_{\mathcal{M}^{*,c}}\|_1 \\
&\leq 4c_u \delta_m^2 + 4\lambda \|\Delta_{\mathcal{M}^*}\|_1 \\
&\leq c_u \delta_m^2 + 4\lambda \sqrt{M^*} \|\Delta^*\|_2.
\end{aligned} \tag{S9}$$

By applying the RE condition, we have

$$\|\Delta^*\|_2 \leq \left\| \frac{1}{\sqrt{\kappa N}} \mathbf{W} \Delta^* \right\|_2. \tag{S10}$$

By plugging (S10) into (S9), we have

$$\begin{aligned}
\frac{1}{N} \|\mathbf{X} \Delta^*\|_2^2 &\leq \frac{16}{3} c_u \delta_m^2 + \lambda \frac{16\sqrt{M^*}}{3\sqrt{\kappa}} \left\| \frac{1}{\sqrt{N}} \mathbf{X} \Delta^* \right\|_2 \\
&\leq C_1 \delta_m^2 + C_2 M^* \lambda^2,
\end{aligned} \tag{S11}$$

where C_1 and C_2 are positive constants. Based on the RE condition, we have

$$\|\Delta^*\|_1^2 \leq \frac{M^*}{\kappa} \frac{1}{N} \|\mathbf{X} \Delta^*\|_2^2 \leq \frac{M^*}{\kappa} (C_1 \delta_m^2 + C_2 M^* \lambda^2),$$

and

$$\|\Delta^*\|_1^2 \leq C_3 \sqrt{M^*} \delta_m + C_4 \sqrt{M^*} \lambda,$$

where C_3 and C_4 are positive constants, and (I) and (II) of the theorem are proved under \mathcal{E}^* .

Let \mathbf{r} be the vector of r_{ij} , since $\mathbf{r} = \mathbf{e} + \tilde{\mathbf{r}}^* - \mathbf{X} \Delta^*$, due to the triangle inequality and

(S11), we have

$$\frac{1}{N}\|\mathbf{r}\| \leq C_5(\delta_m^2 + M^*\lambda^2),$$

which implies $\text{Var}\{E(r_{ij} | i)\} \leq C_5(\delta_m^2 + M\lambda^2)$, and (III) is proved under \mathcal{E}^* .

Finally, we need to choose λ so that $P(\mathcal{E}^*) \rightarrow 1$. For any $t > 0$, we have

$$\begin{aligned} P\left(\frac{2}{N}\|\mathbf{e}^\top \mathbf{X}\|_\infty > t\right) &\leq \sum_{l=1}^p P\left(\frac{2}{N}\mathbf{e}^\top \mathbf{X}_l > t\right) \\ &\leq 2p \exp\left(-\frac{t^2}{8N^{-2}\tilde{\sigma}^2 \max_l \|\mathbf{X}_l\|_2^2}\right) \\ &\leq 2p \exp\left(-\frac{Nt^2}{8C\tilde{\sigma}^2}\right). \end{aligned}$$

Thus, by choosing

$$\lambda = \sqrt{\frac{16C\tilde{\sigma}^2 \log(p)}{N}},$$

we have

$$P(\mathcal{E}^*) = 1 - P\left(\frac{2}{N}\|\mathbf{e}^\top \mathbf{X}\|_\infty > \lambda\right) \geq 1 - 2p^{-1},$$

and the theorem is proved.

B.2 Proof of Theorem 2

Let $\Delta = \hat{\boldsymbol{\theta}} - \boldsymbol{\theta}^0$, we can re-express (2) as

$$\mathbf{Y} = \mathbf{X}\boldsymbol{\beta}^0 + \mathbf{B}\boldsymbol{\gamma}^0 + \mathbf{D}\mathbf{u} + \boldsymbol{\epsilon} = \mathbf{W}\boldsymbol{\theta}^0 + \mathbf{D}\mathbf{u} + \boldsymbol{\epsilon}. \quad (\text{S12})$$

Because

$$\frac{1}{2N} \|\mathbf{Y} - \mathbf{W}\hat{\boldsymbol{\theta}}\|_2^2 + \lambda_1 \|\hat{\boldsymbol{\beta}}\|_1 + \lambda_2 \|\hat{\boldsymbol{\gamma}}\|_1 \leq \frac{1}{2N} \|\mathbf{Y} - \mathbf{W}\boldsymbol{\theta}^0\|_2^2 + \lambda_1 \|\boldsymbol{\beta}^0\|_1 + \lambda_2 \|\boldsymbol{\gamma}^0\|_1,$$

expand $\mathbf{Y} - \mathbf{W}\hat{\boldsymbol{\theta}}$ by $\mathbf{D}\mathbf{u} + \boldsymbol{\epsilon} - \mathbf{W}\boldsymbol{\Delta}$ and plug-in (S12), we have the *basic inequality*:

$$\frac{1}{2N} \|\mathbf{W}\boldsymbol{\Delta}\|_2^2 \leq \frac{1}{N} (\mathbf{D}\mathbf{u} + \boldsymbol{\epsilon})^\top \mathbf{W}\boldsymbol{\Delta} + \lambda_1 (\|\boldsymbol{\beta}^0\|_1 - \|\hat{\boldsymbol{\beta}}\|_1) + \lambda_2 (\|\boldsymbol{\gamma}^0\|_1 - \|\hat{\boldsymbol{\gamma}}\|_1). \quad (\text{S13})$$

By the Holder's inequality, we have

$$\frac{1}{N} (\mathbf{D}\mathbf{u})^\top \mathbf{W}\boldsymbol{\Delta} \leq \left\| \frac{1}{N} (\mathbf{D}\mathbf{u})^\top \mathbf{W} \right\|_\infty \|\boldsymbol{\Delta}\|_1 \leq C\delta_m \|\boldsymbol{\Delta}\|_1, \quad (\text{S14})$$

where $C = \sqrt{c_u}$.

Let \mathcal{E} be the set of events defined as

$$\mathcal{E} = \left\{ \lambda_1 \geq \frac{4}{N} \|\mathbf{X}^\top \boldsymbol{\epsilon}\|_\infty, \lambda_2 \geq \frac{4}{N} \|\mathbf{B}^\top \boldsymbol{\epsilon}\|_\infty \right\},$$

under \mathcal{E} , we have

$$\frac{1}{N} \boldsymbol{\epsilon}^\top \mathbf{W}\boldsymbol{\Delta} \leq \frac{\lambda_1}{4} \|\boldsymbol{\Delta}_\beta\|_1 + \frac{\lambda_2}{4} \|\boldsymbol{\Delta}_\gamma\|_1 \leq \frac{\bar{\lambda}}{4} \|\boldsymbol{\Delta}\|_1, \quad (\text{S15})$$

where $\boldsymbol{\Delta}_\beta = \hat{\boldsymbol{\beta}} - \boldsymbol{\beta}^0$ and $\boldsymbol{\Delta}_\gamma = \hat{\boldsymbol{\gamma}} - \boldsymbol{\gamma}^0$.

Due to the triangle inequality, we have

$$\|\boldsymbol{\beta}^0\|_1 - \|\hat{\boldsymbol{\beta}}\|_1 \leq \|\boldsymbol{\Delta}_{\beta, \mathcal{M}_1}\|_1 - \|\boldsymbol{\Delta}_{\beta, \mathcal{M}_1^c}\|_1$$

and

$$\|\boldsymbol{\gamma}^0\|_1 - \|\hat{\boldsymbol{\gamma}}\|_1 \leq \|\boldsymbol{\Delta}_{\gamma, \mathcal{M}_2}\|_1 - \|\boldsymbol{\Delta}_{\gamma, \mathcal{M}_2^c}\|_1,$$

which implies

$$\lambda_1(\|\boldsymbol{\beta}^0\|_1 - \|\hat{\boldsymbol{\beta}}\|_1) + \lambda_2(\|\boldsymbol{\gamma}^0\|_1 - \|\hat{\boldsymbol{\gamma}}\|_1) \leq \bar{\lambda}(\|\boldsymbol{\Delta}_{\mathcal{M}}\|_1 - \|\boldsymbol{\Delta}_{\mathcal{M}^c}\|_1). \quad (\text{S16})$$

Thus, plugging (S14), (S15), and (S16) into (S13), we have

$$\begin{aligned} \frac{1}{4N} \|\mathbf{W} \boldsymbol{\Delta}\|_2^2 &\leq C\delta_m \|\boldsymbol{\Delta}\|_1 + \frac{\bar{\lambda}}{4} \|\boldsymbol{\Delta}\|_1 + \bar{\lambda}(\|\boldsymbol{\Delta}_{\mathcal{M}}\|_1 - \|\boldsymbol{\Delta}_{\mathcal{M}^c}\|_1) \\ &= \left(\frac{5}{4}\bar{\lambda} + C\delta_m\right) \|\boldsymbol{\Delta}_{\mathcal{M}}\|_1 - \left(\frac{3}{4}\bar{\lambda} - C\delta_m\right) \|\boldsymbol{\Delta}_{\mathcal{M}^c}\|_1. \end{aligned} \quad (\text{S17})$$

For any $e \in (0, 1)$, under (C1), we have $C\delta_m \leq \bar{\lambda}e$ holds with high probability, and

$$\frac{5}{4}\bar{\lambda} + C\delta_m \leq \left(\frac{5}{4} + e\right) \bar{\lambda}, \quad \frac{3}{4}\bar{\lambda} - C\delta_m \geq \left(\frac{3}{4} - e\right) \bar{\lambda},$$

which implies

$$\|\boldsymbol{\Delta}_{\mathcal{M}^c}\|_1 \leq \frac{\frac{5}{4} + e}{\frac{3}{4} - e} \|\boldsymbol{\Delta}_{\mathcal{M}}\|_1.$$

Thus, by choosing $e = 1/8$, we have

$$\|\boldsymbol{\Delta}_{\mathcal{M}^c}\|_1 \leq \frac{11}{5} \|\boldsymbol{\Delta}_{\mathcal{M}}\|_1 \quad (\text{S18})$$

and $\Delta \in \mathcal{C}_{11/5}(\mathcal{M})$. Notice that based on Cauchy-Schwarz inequalities, we have

$$\begin{aligned} \frac{1}{N}(\mathbf{D}\mathbf{r})^\top \mathbf{W}\Delta &\leq \frac{\|\mathbf{D}\mathbf{r}\|_2^2 \|\mathbf{W}\Delta\|_2^2}{\sqrt{N}} \leq \frac{1}{N}\|\mathbf{D}\mathbf{r}\|_2^2 + \frac{1}{4N}\|\mathbf{W}\Delta\|_2^2 \\ &\leq c_u \delta_m^2 + \frac{1}{4N}\|\mathbf{W}\Delta\|_2^2. \end{aligned} \quad (\text{S19})$$

Combining (S17)-(S19), we have

$$\begin{aligned} &\frac{1}{4N}\|\mathbf{W}\Delta\|_2^2 + \bar{\lambda}\|\Delta\|_1 \\ &= \frac{1}{4N}\|\mathbf{W}\Delta\|_2^2 + \bar{\lambda}\|\Delta_{\mathcal{M}}\|_1 + \bar{\lambda}\|\Delta_{\mathcal{M}^c}\|_1 \\ &\leq c_u \delta_m^2 + \bar{\lambda} \left(\frac{9}{4}\|\Delta_{\mathcal{M}}\|_1 + \frac{1}{4}\|\Delta_{\mathcal{M}^c}\|_1 \right) \\ &\leq c_u \delta_m^2 + 3\bar{\lambda}\|\Delta_{\mathcal{M}}\|_1 \\ &\leq c_u \delta_m^2 + 3\bar{\lambda}\sqrt{M}\|\Delta\|_2. \end{aligned} \quad (\text{S20})$$

By applying the RE condition, we have

$$\|\Delta\|_2 \leq \left\| \frac{1}{\sqrt{\kappa N}} \mathbf{W}\Delta \right\|_2. \quad (\text{S21})$$

By plugging (S21) into (S20), we have

$$\begin{aligned} \frac{1}{N}\|\mathbf{W}\Delta\|_2^2 &\leq 4c_u \delta_m^2 + \bar{\lambda} \frac{3\sqrt{M}}{4\sqrt{\kappa}} \left\| \frac{1}{\sqrt{N}} \mathbf{W}\Delta \right\|_2 \\ &\leq C_1 \delta_m^2 + C_2 M \bar{\lambda}, \end{aligned} \quad (\text{S22})$$

where C_1 and C_2 are positive constants. Based on the RE condition, we have

$$\|\Delta\|_1^2 \leq \frac{M}{\kappa} \frac{1}{N} \|\mathbf{W}\Delta\|_2^2 \leq \frac{M}{\kappa} (C_1 \delta_m^2 + C_2 M \bar{\lambda}),$$

and

$$\|\Delta\|_1 \leq C_3\sqrt{M}\delta_m + C_4M\bar{\lambda},$$

where C_3 and C_4 are positive constants.

We need choose λ_1 and λ_2 so that $P(\mathcal{E}) \rightarrow 1$. For each \mathbf{X}_k , due to (C3), for any $t > 0$, we have

$$P\left(\frac{1}{N}|\mathbf{X}_k^\top \boldsymbol{\epsilon}| > t\right) \leq 2 \exp\left(-N\frac{t^2}{2\sigma^2}\right).$$

Applying the union bound over p , we have

$$P(\mathcal{E}_X^c) \leq 2p \exp\left(-N\frac{\lambda_1^2}{32\sigma^2}\right).$$

Similarly, we have

$$P(\mathcal{E}_B^c) \leq 2p_0 \exp\left(-N\frac{\lambda_2^2}{32\sigma^2}\right),$$

and the theorem is proved for $p, p_0 \rightarrow \infty$.

B.3 Proof of Theorem 4

Based on the optimality of $\hat{\boldsymbol{\theta}}$, let $\Delta = \hat{\boldsymbol{\theta}} - \tilde{\boldsymbol{\theta}}$ and $R(\boldsymbol{\theta}) = \lambda_1\|\boldsymbol{\beta}\|_1 + \lambda_2\|\boldsymbol{\gamma}\|_1$, we have

$$\mathcal{L}_N(\tilde{\boldsymbol{\theta}} + \Delta) - \mathcal{L}_N(\tilde{\boldsymbol{\theta}}) \leq R(\tilde{\boldsymbol{\theta}}) - R(\tilde{\boldsymbol{\theta}} + \Delta). \quad (\text{S23})$$

Define \mathcal{E} be the set of events defined as

$$\mathcal{E} = \{\bar{\lambda}/2 \geq \|\nabla \mathcal{L}_N(\boldsymbol{\theta}^0)\|_\infty\}.$$

Due to (G2) and (13), we have $P(\mathcal{E}) \rightarrow 1$ as $p, p_0 \rightarrow \infty$. By Holder's inequality, under \mathcal{E} , we have

$$|\langle \nabla \mathcal{L}_N(\tilde{\boldsymbol{\theta}}), \boldsymbol{\Delta} \rangle| \leq \|\nabla \mathcal{L}_N(\tilde{\boldsymbol{\theta}})\|_\infty \|\boldsymbol{\Delta}\|_1 \leq \frac{\bar{\lambda}}{2} \|\boldsymbol{\Delta}\|_1. \quad (\text{S24})$$

By adding and subtracting $\langle \nabla \mathcal{L}_N(\tilde{\boldsymbol{\theta}}), \boldsymbol{\Delta} \rangle$ on (S23), similar to the proof of Theorem 1, under \mathcal{E} , we have

$$\mathcal{L}_N(\tilde{\boldsymbol{\theta}} + \boldsymbol{\Delta}) - \mathcal{L}_N(\tilde{\boldsymbol{\theta}}) - \langle \nabla \mathcal{L}_N(\boldsymbol{\theta}^0), \boldsymbol{\Delta} \rangle \leq \frac{3}{2} \bar{\lambda} \|\boldsymbol{\Delta}_{\mathcal{M}}\|_1 - \frac{1}{2} \bar{\lambda} \|\boldsymbol{\Delta}_{\mathcal{M}^c}\|_1. \quad (\text{S25})$$

On the other hand, by Taylor expansion and (G1), we have

$$\begin{aligned} \mathcal{L}_N(\tilde{\boldsymbol{\theta}} + \boldsymbol{\Delta}) - \mathcal{L}_N(\tilde{\boldsymbol{\theta}}) - \langle \nabla \mathcal{L}_N(\tilde{\boldsymbol{\theta}}), \boldsymbol{\Delta} \rangle &= \frac{1}{2N} \sum_{i,j} \ell''(\tilde{\xi}_{ij}, y_{ij}) (\mathbf{W}_{ij}^\top \boldsymbol{\Delta})^2 + o(N^{-1}) \\ &\geq \frac{C_l}{2N} \|\mathbf{W} \boldsymbol{\Delta}\|_2^2. \end{aligned} \quad (\text{S26})$$

Thus, combining (S25) and (S26), we have

$$\frac{C_l}{2N} \|\mathbf{W} \boldsymbol{\Delta}\|_2^2 \leq \frac{3}{2} \bar{\lambda} \|\boldsymbol{\Delta}_{\mathcal{M}}\|_1 - \frac{1}{2} \bar{\lambda} \|\boldsymbol{\Delta}_{\mathcal{M}^c}\|_1,$$

which implies $\Delta \in \mathcal{C}_3(\mathcal{M})$. Thus, we have

$$\begin{aligned} & \frac{C_l}{2N} \|\mathbf{W} \Delta\|_2^2 + \bar{\lambda} \|\Delta\|_1 \\ & \leq \bar{\lambda} \left(\frac{5}{2} \|\Delta_{\tilde{\mathcal{M}}}\|_1 + \frac{1}{2} \|\Delta_{\tilde{\mathcal{M}}^c}\|_1 \right) \\ & \leq 4\bar{\lambda} \|\Delta_{\tilde{\mathcal{M}}}\|_1 \leq 4\bar{\lambda} \sqrt{\tilde{M}} \|\Delta\|_2, \end{aligned}$$

and based on the RE condition, the theorem can be proved.

B.4 Proof of Theorem 5

Based on the definition of $\tilde{\boldsymbol{\theta}}_\delta$, by applying Taylor expansion on $\nabla \mathcal{L}_\delta(\boldsymbol{\theta})$, we have

$$0 = \nabla \mathcal{L}_\delta(\tilde{\boldsymbol{\theta}}_\delta) \approx \nabla \mathcal{L}_\delta(\boldsymbol{\theta}^0) + \nabla^2 \mathcal{L}_\delta(\boldsymbol{\theta}^0)(\tilde{\boldsymbol{\theta}}_\delta - \boldsymbol{\theta}^0),$$

which implies

$$\tilde{\boldsymbol{\theta}}_\delta - \boldsymbol{\theta}^0 \approx -[\nabla^2 \mathcal{L}_\delta(\boldsymbol{\theta}^0)]^{-1} \nabla \mathcal{L}_\delta(\boldsymbol{\theta}^0).$$

Under (G3), we have

$$\|\tilde{\boldsymbol{\theta}}_\delta - \boldsymbol{\theta}^0\|_2 \leq C \|\nabla \mathcal{L}_\delta(\boldsymbol{\theta}^0)\|_2,$$

where $C > 0$. Due to the Lipschitzness of l' , we have

$$\|\nabla \mathcal{L}_\delta(\boldsymbol{\theta}^0)\|_2 = \|\mathbb{E}_\delta[\nabla \ell(W^\top \boldsymbol{\theta}^0; Y_{ij})] - \mathbb{E}_0[\nabla \ell(W^\top \boldsymbol{\theta}^0; Y_{ij})]\|_2 \leq C' \delta_m,$$

where $C' > 0$, and the theorem is proved.

B.5 Proof of Proposition 1

Let

$$\tilde{\mathbf{Y}} = \mathbf{W}\boldsymbol{\theta}^0 + \boldsymbol{\epsilon} = \boldsymbol{\mu}_0 + \boldsymbol{\epsilon}, \quad \mathbf{Y} = \tilde{\mathbf{Y}} + \mathbf{D}\mathbf{u},$$

we have

$$\boldsymbol{\eta}_l^\top \tilde{\mathbf{Y}} \sim N(\boldsymbol{\eta}_l^\top \boldsymbol{\mu}_0, \sigma^2 \|\boldsymbol{\eta}_l\|_2^2), \quad \boldsymbol{\eta}_l^\top \mathbf{Y} \sim N(\boldsymbol{\eta}_l^\top \boldsymbol{\mu}_0 + \boldsymbol{\eta}_l^\top \mathbf{D}\mathbf{u}, \sigma^2 \|\boldsymbol{\eta}_l\|_2^2). \quad (\text{S27})$$

The total variation distance, denoted as $d_{TV}(\cdot, \cdot)$, between the normal distributions defined in (S27) is upper-bounded by $|\boldsymbol{\eta}_l^\top \mathbf{D}\mathbf{u}| = O(\sqrt{N}\delta_m/\sigma)$. Thus,

$$d_{TV}(\boldsymbol{\eta}_l^\top \tilde{\mathbf{Y}}, \boldsymbol{\eta}_l^\top \mathbf{Y}) = O(\sqrt{N}\delta_m/\sigma).$$

Due to (8), conditioning on the selection event $\{\mathcal{M}, \mathbf{s}\}$ is equivalent to conditioning on a convex set. Since the conditional densities of Gaussian measures truncated to a convex set are Lipschitz in the mean parameter (Fithian et al., 2014), we have

$$d_{TV}(\boldsymbol{\eta}_l^\top \tilde{\mathbf{Y}} | (\mathcal{M}, \mathbf{s}), \boldsymbol{\eta}_l^\top \mathbf{Y} | (\mathcal{M}, \mathbf{s})) = O(\sqrt{N}\delta_m/\sigma). \quad (\text{S28})$$

Furthermore, let $\tilde{T}^l = T_{\phi_l, \sigma^2 \|\boldsymbol{\eta}_l\|_2^2}^{[L(\mathbf{s}), U(\mathbf{s})]}(\boldsymbol{\eta}_l^\top \mathbf{Y}^0)$, since the pivot statistic is a smooth function of the conditional CDF, the Kolmogorov distance between T^l and \tilde{T}^l remains the same order, and the proposition is proved.

B.6 Proof of Theorem 6

The first-order Taylor expansion of $\nabla\mathcal{L}_N(\tilde{\boldsymbol{\theta}}_\delta)$ at $\hat{\boldsymbol{\theta}}$ gives

$$\nabla\mathcal{L}_N(\tilde{\boldsymbol{\theta}}_\delta) = \nabla\mathcal{L}_N(\hat{\boldsymbol{\theta}}) + \nabla^2\mathcal{L}_N(\bar{\boldsymbol{\theta}}_\delta)(\hat{\boldsymbol{\theta}} - \tilde{\boldsymbol{\theta}}_\delta), \quad (\text{S29})$$

where $\bar{\boldsymbol{\theta}}_\delta$ lies between $\tilde{\boldsymbol{\theta}}_\delta$ and $\hat{\boldsymbol{\theta}}$. By multiplying $\hat{\mathbf{a}}_l$ on both sides of (S29), [Van de Geer et al. \(2014\)](#) showed that

$$\hat{\beta}_l^1 - \tilde{\beta}_{\delta,l} = -\hat{\mathbf{a}}_l^\top \nabla\mathcal{L}_N(\tilde{\boldsymbol{\theta}}_\delta) + (\mathbf{e}_l^\top - \hat{\mathbf{a}}_l^\top \nabla^2\mathcal{L}_N(\bar{\boldsymbol{\theta}}_\delta)) (\hat{\boldsymbol{\theta}} - \tilde{\boldsymbol{\theta}}_\delta). \quad (\text{S30})$$

Denote the second term of (S30) as R_l , under regularity condition (C6) and the consistency of $\hat{\boldsymbol{\theta}}$ derived in Theorem 3, we have

$$\sqrt{m}|R_j| \leq \sqrt{m}\|\mathbf{e}_l - \nabla^2\mathcal{L}_N(\bar{\boldsymbol{\theta}}_\delta)\hat{\mathbf{a}}_l\|_\infty\|\hat{\boldsymbol{\theta}} - \tilde{\boldsymbol{\theta}}_\delta\|_1 = o_p(1). \quad (\text{S31})$$

Under the canonical generalized linear regression model assumed in Section 3, we have

$$-\hat{\mathbf{a}}_l^\top \nabla\mathcal{L}_N(\tilde{\boldsymbol{\theta}}_\delta) = \frac{1}{N} \sum_{i,j} \phi_{l,ij} + (\mathbf{a}_l^0 - \hat{\mathbf{a}}_l)^\top \nabla\mathcal{L}_N(\tilde{\boldsymbol{\theta}}_\delta).$$

Similarly, under (C6), the second term is $o_p(N^{-1/2})$. Combining with (S31), to complete the proof of part (I) of the theorem, it is sufficient to show that $\frac{1}{N} \sum_{i,j} \phi_{l,ij} = \frac{1}{m} \sum_{j=1}^m \Phi_{l,i} + o_p(m^{-1/2})$. Since cluster sizes are uniformly bounded by (C2), we have $m/c_u \leq N \leq m/c_l$. Hence, replacing N by m only changes the leading term by a multiplicative constant, i.e.,

$$\hat{\beta}_l^1 - \tilde{\beta}_{\delta,l} = \frac{1}{m} \sum_{i=1}^m \Phi_{l,i} + o_p(m^{-1/2}),$$

which proofs part (I) of the theorem.

Due to the independence of $\Phi_{l,i}$, the Lyapunov central limit theorem (Billingsley, 2013) can be directly applied to prove part (II) of the theorem.

Finally, because

$$\text{Var}(\hat{V}_l) = \frac{1}{m^2} \sum_{i=1}^m \text{Var}(\hat{\Phi}_{l,i}^2) \leq \frac{1}{m^2} \sum_{i=1}^m \text{E}(\Phi_{l,i}^4) \leq \frac{C}{m} \rightarrow 0,$$

by Chebyshev's inequality, part (III) of the theorem is proved.

C Additional details for selective inference with SHEL

C.1 Polyhedral representation of the SHEL selection event

This section provides the technical details underlying the selective-inference procedure in Section 4.1. Recall that the weighted SHEL estimator can be rewritten as a standard LASSO problem by defining

$$\mathbf{Z} = \mathbf{W} \text{diag}(\mathbf{a}^{-1}), \quad \boldsymbol{\phi} = \text{diag}(\mathbf{a})\boldsymbol{\theta},$$

where $\mathbf{a} = (a_1, \dots, a_{p+p_0})^\top$ is the penalty-weight vector. Then

$$\hat{\boldsymbol{\phi}} = \arg \min_{\boldsymbol{\phi} \in \mathbb{R}^{p+p_0}} \left\{ \frac{1}{2N} \|\mathbf{Y} - \mathbf{Z}\boldsymbol{\phi}\|_2^2 + \lambda_1 \|\boldsymbol{\phi}\|_1 \right\}.$$

Let $\hat{\mathcal{M}} = \text{supp}(\hat{\boldsymbol{\phi}})$ denote the active set, and let $\hat{\mathbf{s}}$ denote the corresponding sign vector, where $\hat{s}_k = \text{sign}(\hat{\phi}_k)$ for $k \in \hat{\mathcal{M}}$ and $\hat{s}_k \in [-1, 1]$ for $k \in \hat{\mathcal{M}}^c$. The KKT conditions for the

LASSO require

$$\frac{1}{N} \mathbf{Z}^\top (\mathbf{Y} - \mathbf{Z} \hat{\boldsymbol{\phi}}) - \lambda_1 \hat{\mathbf{s}} = 0. \quad (\text{S32})$$

Fix an active set \mathcal{M} and sign vector \mathbf{s} . Let

$$\hat{\boldsymbol{\Sigma}}_{\mathcal{M}} = \frac{1}{N} \mathbf{Z}_{\mathcal{M}}^\top \mathbf{Z}_{\mathcal{M}}, \quad \mathcal{P}_{\mathcal{M}} = \mathbf{Z}_{\mathcal{M}} (\mathbf{Z}_{\mathcal{M}}^\top \mathbf{Z}_{\mathcal{M}})^{-1} \mathbf{Z}_{\mathcal{M}}^\top,$$

where $\mathcal{P}_{\mathcal{M}}$ is the projection matrix onto the column space of $\mathbf{Z}_{\mathcal{M}}$. Standard LASSO theory (Lee et al., 2016, Theorem 4.3) shows that the event

$$\{\hat{\mathcal{M}} = \mathcal{M}, \hat{\mathbf{s}}_{\mathcal{M}} = \mathbf{s}\}$$

can be expressed as a polyhedron in the data space:

$$\{\hat{\mathcal{M}} = \mathcal{M}, \hat{\mathbf{s}}_{\mathcal{M}} = \mathbf{s}\} = \{\mathbf{A}(\mathcal{M}, \mathbf{s}) \mathbf{Y} \leq \mathbf{b}(\mathcal{M}, \mathbf{s})\}, \quad (\text{S33})$$

where

$$\mathbf{A}(\mathcal{M}, \mathbf{s}) = \begin{pmatrix} \mathbf{A}_0(\mathcal{M}, \mathbf{s}) \\ \mathbf{A}_1(\mathcal{M}, \mathbf{s}) \end{pmatrix}, \quad \mathbf{b}(\mathcal{M}, \mathbf{s}) = \begin{pmatrix} \mathbf{b}_0(\mathcal{M}, \mathbf{s}) \\ \mathbf{b}_1(\mathcal{M}, \mathbf{s}) \end{pmatrix},$$

with

$$\begin{aligned}\mathbf{A}_0(\mathcal{M}, \mathbf{s}) &= \begin{pmatrix} \frac{1}{\lambda_1 N} \mathbf{Z}_{\mathcal{M}^c}^\top (\mathbf{I}_N - \mathcal{P}_{\mathcal{M}}) \\ -\frac{1}{\lambda_1 N} \mathbf{Z}_{\mathcal{M}^c}^\top (\mathbf{I}_N - \mathcal{P}_{\mathcal{M}}) \end{pmatrix}, \\ \mathbf{b}_0(\mathcal{M}, \mathbf{s}) &= \begin{pmatrix} \mathbf{1} - \frac{1}{N} \mathbf{Z}_{\mathcal{M}^c}^\top \mathbf{Z}_{\mathcal{M}} \hat{\Sigma}_{\mathcal{M}}^{-1} \mathbf{s} \\ \mathbf{1} + \frac{1}{N} \mathbf{Z}_{\mathcal{M}^c}^\top \mathbf{Z}_{\mathcal{M}} \hat{\Sigma}_{\mathcal{M}}^{-1} \mathbf{s} \end{pmatrix}, \\ \mathbf{A}_1(\mathcal{M}, \mathbf{s}) &= -\frac{1}{N} \text{diag}(\mathbf{s}) \hat{\Sigma}_{\mathcal{M}}^{-1} \mathbf{Z}_{\mathcal{M}}^\top, \\ \mathbf{b}_1(\mathcal{M}, \mathbf{s}) &= -\lambda_1 \text{diag}(\mathbf{s}) \hat{\Sigma}_{\mathcal{M}}^{-1} \mathbf{s}.\end{aligned}$$

Here, $\mathbf{1}$ denotes a conformable vector of ones. For notational simplicity, in the sequel we write \mathbf{A} and \mathbf{b} in place of $\mathbf{A}(\mathcal{M}, \mathbf{s})$ and $\mathbf{b}(\mathcal{M}, \mathbf{s})$, respectively.

C.2 Conditional law under polyhedral selection

Let $\boldsymbol{\eta} \in \mathbb{R}^N$ be any contrast vector. Under the Gaussian model

$$\mathbf{Y} \sim N(\boldsymbol{\mu}, \boldsymbol{\Sigma}),$$

the polyhedral lemma in [Lee et al. \(2016\)](#) implies that

$$[\boldsymbol{\eta}^\top \mathbf{Y} \mid \{\mathbf{A}\mathbf{Y} \leq \mathbf{b}\}] \sim TN(\boldsymbol{\eta}^\top \boldsymbol{\mu}, \boldsymbol{\eta}^\top \boldsymbol{\Sigma} \boldsymbol{\eta}, L, U),$$

where $TN(\mu, \sigma^2, a, b)$ denotes the $N(\mu, \sigma^2)$ distribution truncated to $[a, b]$. Its cumulative distribution function is

$$T_{\mu, \sigma^2}^{[a, b]}(x) = \frac{\Phi\left(\frac{x-\mu}{\sigma}\right) - \Phi\left(\frac{a-\mu}{\sigma}\right)}{\Phi\left(\frac{b-\mu}{\sigma}\right) - \Phi\left(\frac{a-\mu}{\sigma}\right)}. \quad (\text{S34})$$

To define the truncation limits, let

$$\mathbf{c} = \Sigma \boldsymbol{\eta} (\boldsymbol{\eta}^\top \Sigma \boldsymbol{\eta})^{-1}, \quad \mathbf{f} = (\mathbf{I}_N - \mathbf{c} \boldsymbol{\eta}^\top) \mathbf{Y}.$$

Then the truncation interval is given by

$$L = \max_{k: (\mathbf{A}\mathbf{c})_k < 0} \frac{b_k - (\mathbf{A}\mathbf{f})_k}{(\mathbf{A}\mathbf{c})_k},$$

$$U = \min_{k: (\mathbf{A}\mathbf{c})_k > 0} \frac{b_k - (\mathbf{A}\mathbf{f})_k}{(\mathbf{A}\mathbf{c})_k}.$$

These expressions follow directly from decomposing $\mathbf{Y} = \mathbf{c}(\boldsymbol{\eta}^\top \mathbf{Y}) + \mathbf{f}$ and translating the event $\mathbf{A}\mathbf{Y} \leq \mathbf{b}$ into linear constraints on the scalar $\boldsymbol{\eta}^\top \mathbf{Y}$.

C.3 Selective pivot for SHEL

In the main text, we consider inference for a selected coordinate of the reparameterized coefficient vector $\boldsymbol{\phi}$. For $l \in \mathcal{M}$, define

$$\boldsymbol{\eta}_l = \mathbf{Z}_{\mathcal{M}} (\mathbf{Z}_{\mathcal{M}}^\top \mathbf{Z}_{\mathcal{M}})^{-1} \mathbf{e}_l,$$

where \mathbf{e}_l is the unit vector selecting the l th coordinate within the active set. Under the working model

$$\mathbf{Y} = \mathbf{Z}\boldsymbol{\phi}^0 + \boldsymbol{\epsilon}, \quad \boldsymbol{\epsilon} \sim N(0, \sigma^2 \mathbf{I}_N),$$

the selective pivot is

$$T^l = T_{\phi_l, \sigma^2 \|\boldsymbol{\eta}_l\|_2^2}^{[L, U]}(\boldsymbol{\eta}_l^\top \mathbf{Y}).$$

Conditional on the event $\{\hat{\mathcal{M}} = \mathcal{M}, \hat{\mathbf{s}}_{\mathcal{M}} = \mathbf{s}\}$, this pivot is exactly uniformly distributed on $(0, 1)$ under the null hypothesis for ϕ_j .

A $(1 - \alpha)$ -confidence interval for ϕ_l can therefore be obtained by inverting the pivot, that is, by collecting all values of ϕ_l that are not rejected by the corresponding selective test at level α .

C.4 Approximate validity under small synthetic-approximation error

When the sparse synthetic approximation (SSA) condition holds and the approximation error δ_m is small but not exactly zero, the selective pivot above is no longer exactly uniform. However, its deviation from uniformity is controlled by the size of the residual approximation error. Specifically, under the conditions of Proposition 1,

$$\sup_{x \in [0, 1]} \left| P\{T^l \leq x \mid (\mathcal{M}, \mathbf{s})\} - x \right| \leq C \frac{\sqrt{N} \delta_m}{\sigma} + o(1)$$

for some constant $C > 0$. Hence, the pivot remains asymptotically valid whenever $\delta_m = o_p(N^{-1/2})$.

The proof follows by comparing the conditional distribution of $\boldsymbol{\eta}_l^\top \mathbf{Y}$ under the true model with that under the ideal Gaussian working model and then bounding the induced perturbation of the truncated Gaussian pivot. Since the argument is technical and follows standard perturbation steps, we omit the details here.

C.5 Extension to clustered Gaussian errors under the SSE condition

When the approximation error is not negligible, exact selective inference under an i.i.d. Gaussian working model is no longer appropriate. Under the sufficient sparse exogeneity (SSE) condition, however, if we additionally assume

$$u_i \sim N(0, \tau^2),$$

then the model can be written as

$$\mathbf{Y} = \mathbf{W}\boldsymbol{\theta}^0 + \tilde{\boldsymbol{\epsilon}}, \quad \tilde{\boldsymbol{\epsilon}} = \mathbf{D}\mathbf{u} + \boldsymbol{\epsilon},$$

where

$$\tilde{\boldsymbol{\epsilon}} \sim N(0, \boldsymbol{\Omega}), \quad \boldsymbol{\Omega} = \sigma^2 \mathbf{I}_N + \tau^2 \mathbf{D}\mathbf{D}^\top.$$

Thus, the response remains Gaussian, but with clustered covariance. In this case the same polyhedral selective-inference argument applies after replacing the covariance matrix in the pivot by $\boldsymbol{\Omega}$:

$$T^l = T_{\phi_l, \boldsymbol{\eta}_l^\top \boldsymbol{\Omega} \boldsymbol{\eta}_l}^{[L, U]}(\boldsymbol{\eta}_l^\top \mathbf{Y}).$$

Therefore, the selective pivot remains exact provided the covariance structure is known and correctly specified.

C.6 Conditioning on the active set versus conditioning on the sign pattern

The polyhedral framework can be implemented either by conditioning on the full event

$$\{\hat{\mathcal{M}} = \mathcal{M}, \hat{\mathbf{s}}_{\mathcal{M}} = \mathbf{s}\},$$

or by conditioning only on the active set $\{\hat{\mathcal{M}} = \mathcal{M}\}$ and integrating over all sign vectors compatible with \mathcal{M} (Lee et al., 2016). The latter approach is generally less conservative and can yield more powerful inference. However, it requires handling a union of polyhedra, which may be computationally burdensome when the active set is moderate or large (Tibshirani et al., 2016; Le Duy and Takeuchi, 2021). For computational simplicity, we therefore condition on both the active set and the sign vector throughout this article.

D Algorithms

Algorithm 1 Synthetic heterogeneous-effects LASSO (SHEL) and generalized synthetic heterogeneous-effects LASSO (GSHEL).

- 1: Set significance level α
 - 2: $j \leftarrow 1$
 - 3: **for** $l = 1, \dots, p$ **do**
 - 4: **if** X_l is continuous **then**
 - 5: Perform an ANOVA
 - 6: **else if** X_l is categorical **then**
 - 7: Fit a generalized random-intercepts model
 - 8: Test whether the between-cluster variance is zero
 - 9: **end if**
 - 10: **if** p-value $< \alpha$ **then**
 - 11: Compute the cluster means of X_l , denoted by $\bar{\mathbf{X}}_l$
 - 12: $\mathbf{B}_{.j} \leftarrow \bar{\mathbf{X}}_l; j \leftarrow j + 1$
 - 13: **end if**
 - 14: **end for**
 - 15: $p_0 \leftarrow j - 1$
 - 16: Fit (18) or (19), with λ_1 selected by K -fold cross-validation
 - 17: For SHEL, apply the selective-inference procedure
 - 18: For GSHEL, apply either the selective inference or the debiased inference procedure
-

Algorithm 2 Iterative synthetic heterogeneous-effects LASSO (ISHEL) and generalized synthetic heterogeneous-effects LASSO (IGSHEL).

- 1: Run Algorithm 1 without the inference step
 - 2: Initialize $\widehat{\mathbf{D}\boldsymbol{\alpha}}^{(0)} \leftarrow \mathbf{B}\hat{\boldsymbol{\gamma}}^{(0)}$
 - 3: Set convergence threshold e_{thr} ; set $e \leftarrow \infty$ and $s \leftarrow 1$
 - 4: **while** $e \geq e_{\text{thr}}$ **do**
 - 5: Augment the design matrix with $\widehat{\mathbf{D}\boldsymbol{\alpha}}^{(s-1)}$
 - 6: Fit (18) or (19), with λ_1 selected by K -fold cross-validation
 - 7: Update $\widehat{\mathbf{D}\boldsymbol{\alpha}}^{(s)} \leftarrow \mathbf{B}\hat{\boldsymbol{\gamma}}^{(s)}$
 - 8: $e \leftarrow \left\| \widehat{\mathbf{D}\boldsymbol{\alpha}}^{(s)} - \widehat{\mathbf{D}\boldsymbol{\alpha}}^{(s-1)} \right\|_2^2$
 - 9: $s \leftarrow s + 1$
 - 10: **end while**
-

E Additional simulation results

E.1 Definitions of performance measures

Table S1: Measures of performance in simulation studies.

Metrics	Definition
False positives	the number of selected covariates that corresponded to the zero coefficients
True positives	the number of selected covariates that correspond to the nonzero coefficients
Root mean squared error	square root of the quadratic mean of the differences between Y_{ij} and \hat{Y}_{ij}
Residue ICC	residue intraclass correlation, obtained by fitting a random-intercept model on the fitted residuals
False positive rate	the proportion of zero coefficients, selected by SHEL or GSHEL, is tested significant at a significance level of 0.05
Sensitivity	sensitivity of in-sample prediction
Specificity	specificity of in-sample prediction
Power	the proportion of nonzero coefficients is tested significant at a significance level of 0.05
Median CI length	median length of the 95% confidence intervals for variables selected by SHEL or GSHEL

E.2 Additional simulation results for variable selection, parameter estimation, and prediction

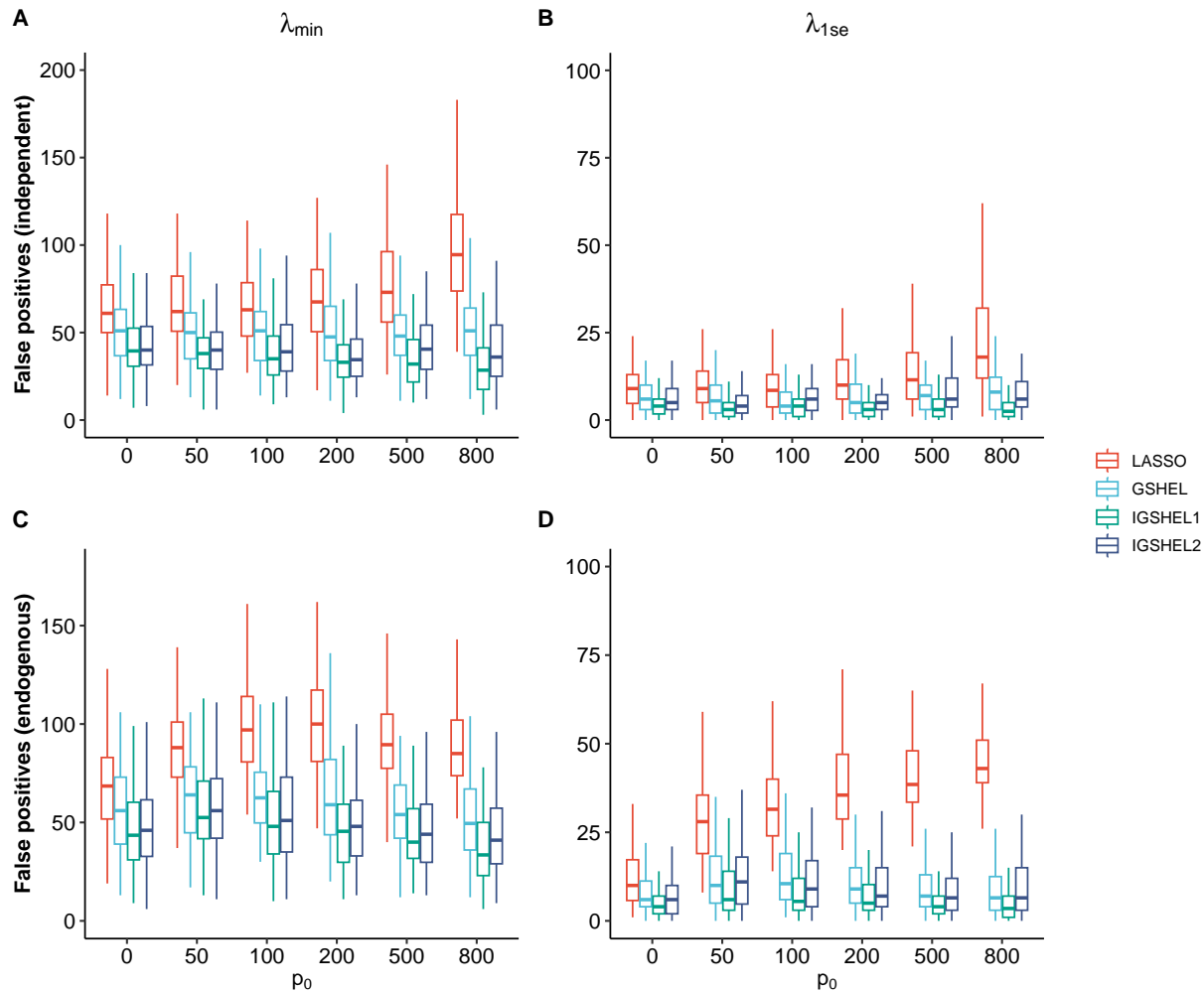


Figure S1: Number of false selections in high-dimensional logistic random-intercepts models with Gaussian random intercepts.

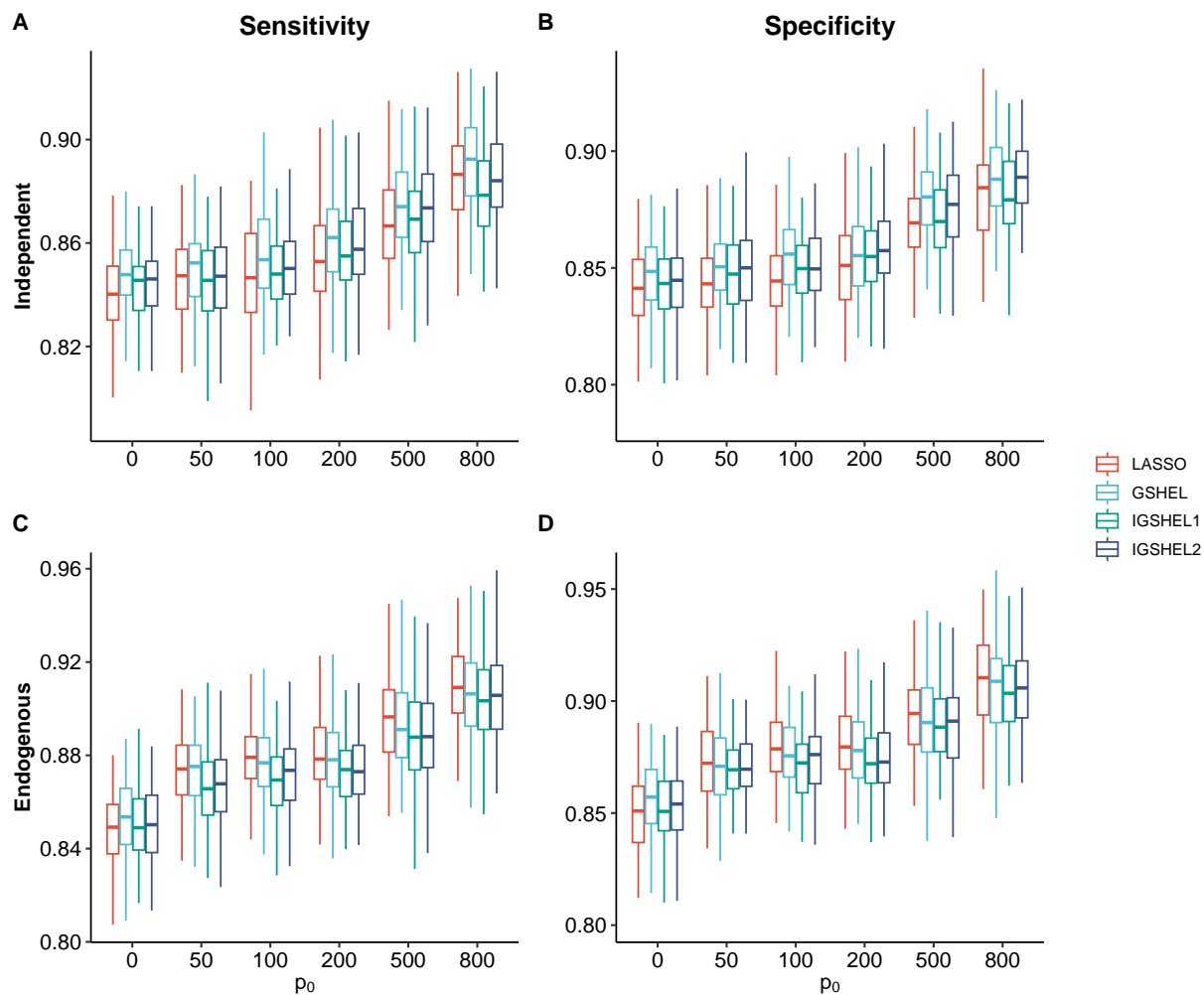


Figure S2: Sensitivity and specificity in high-dimensional logistic random-intercepts models with Gaussian random intercepts.

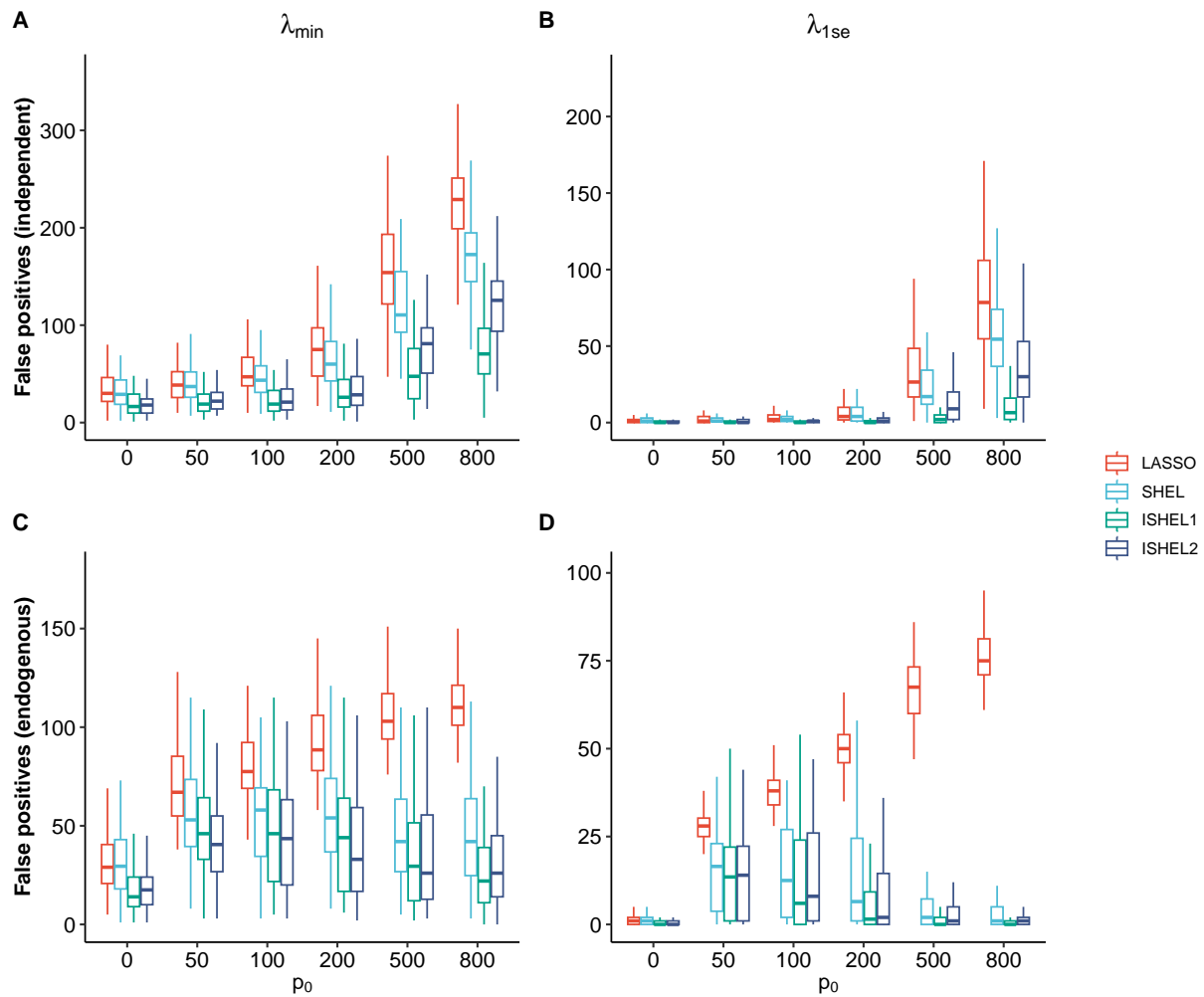


Figure S3: Number of false selections for high-dimensional linear random-effects models with Gaussian mixture random intercepts.

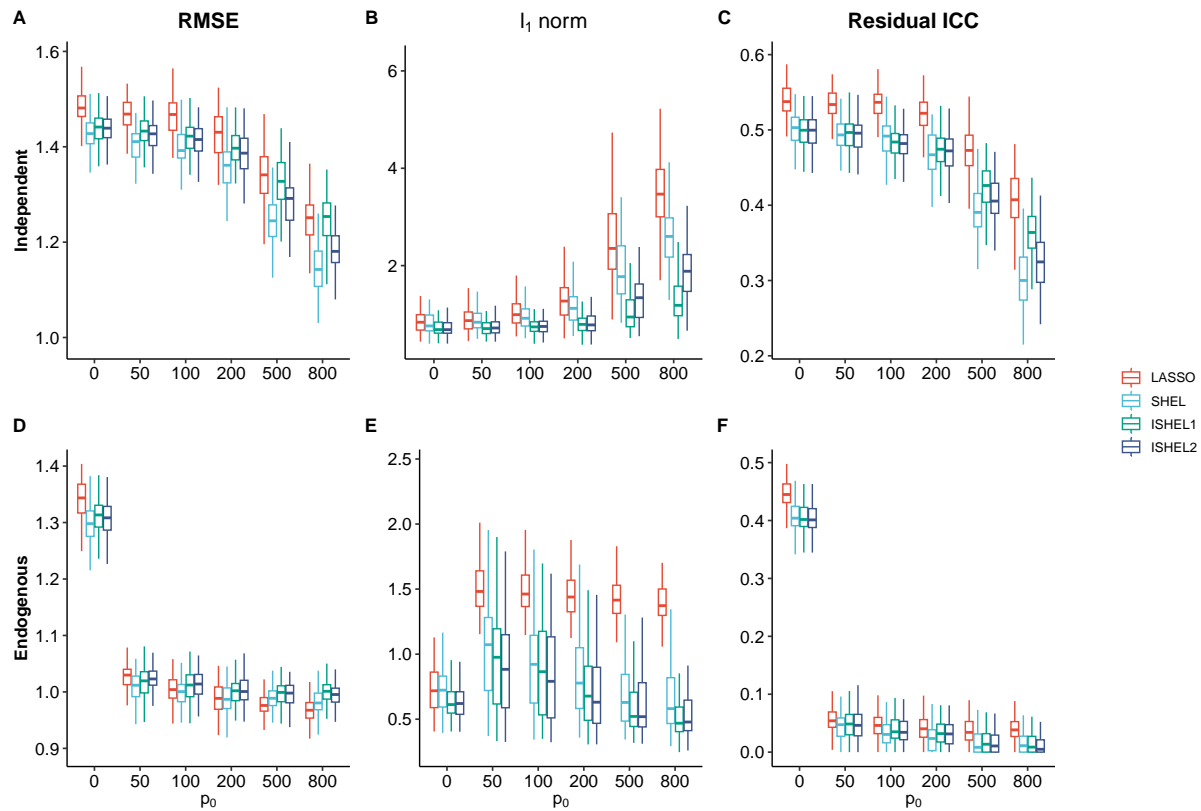


Figure S4: Empirical RMSE, $\|\hat{\beta} - \beta^0\|_1$, and residual ICC in high-dimensional linear random-intercepts models with Gaussian mixture random intercepts.

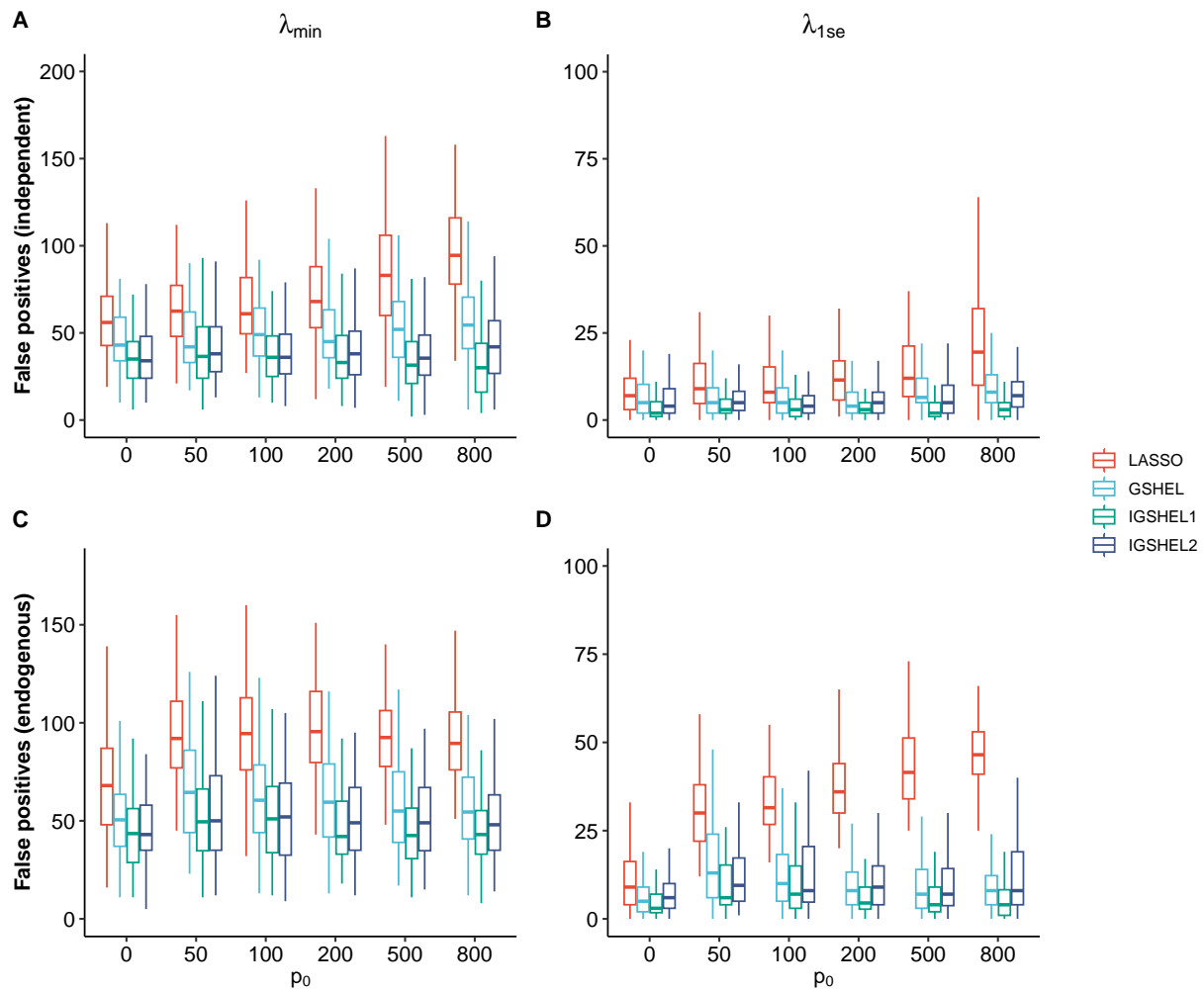


Figure S5: Number of false selections in high-dimensional logistic random-intercepts models with Gaussian mixture random intercepts.

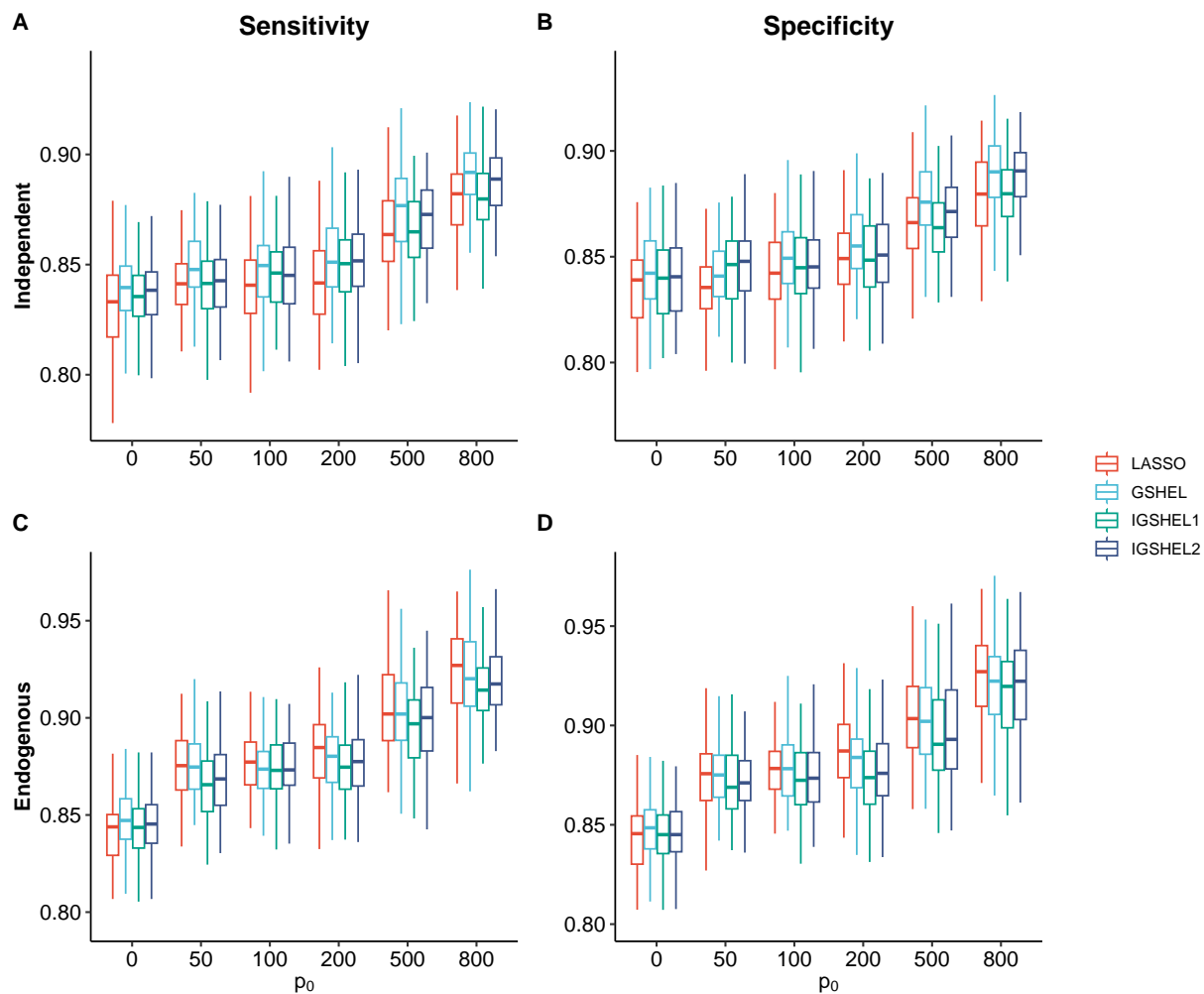


Figure S6: Sensitivity and specificity in high-dimensional logistic random-intercepts models with Gaussian mixture random intercepts.

E.3 Additional simulation results for post-selection inference

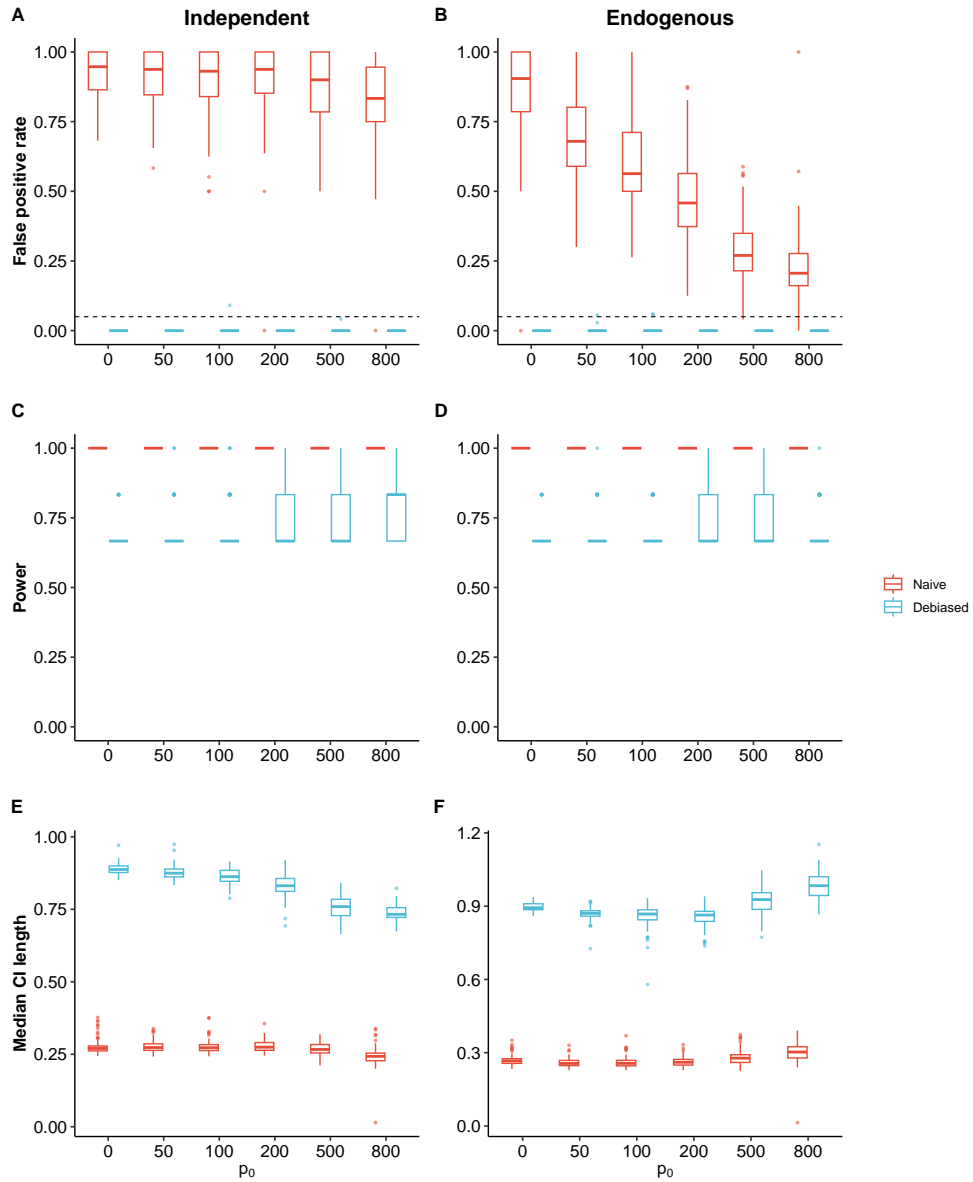


Figure S7: False positive rate, power, and median 95% CI length for Gaussian random intercepts, with variables selected from GSHEL.

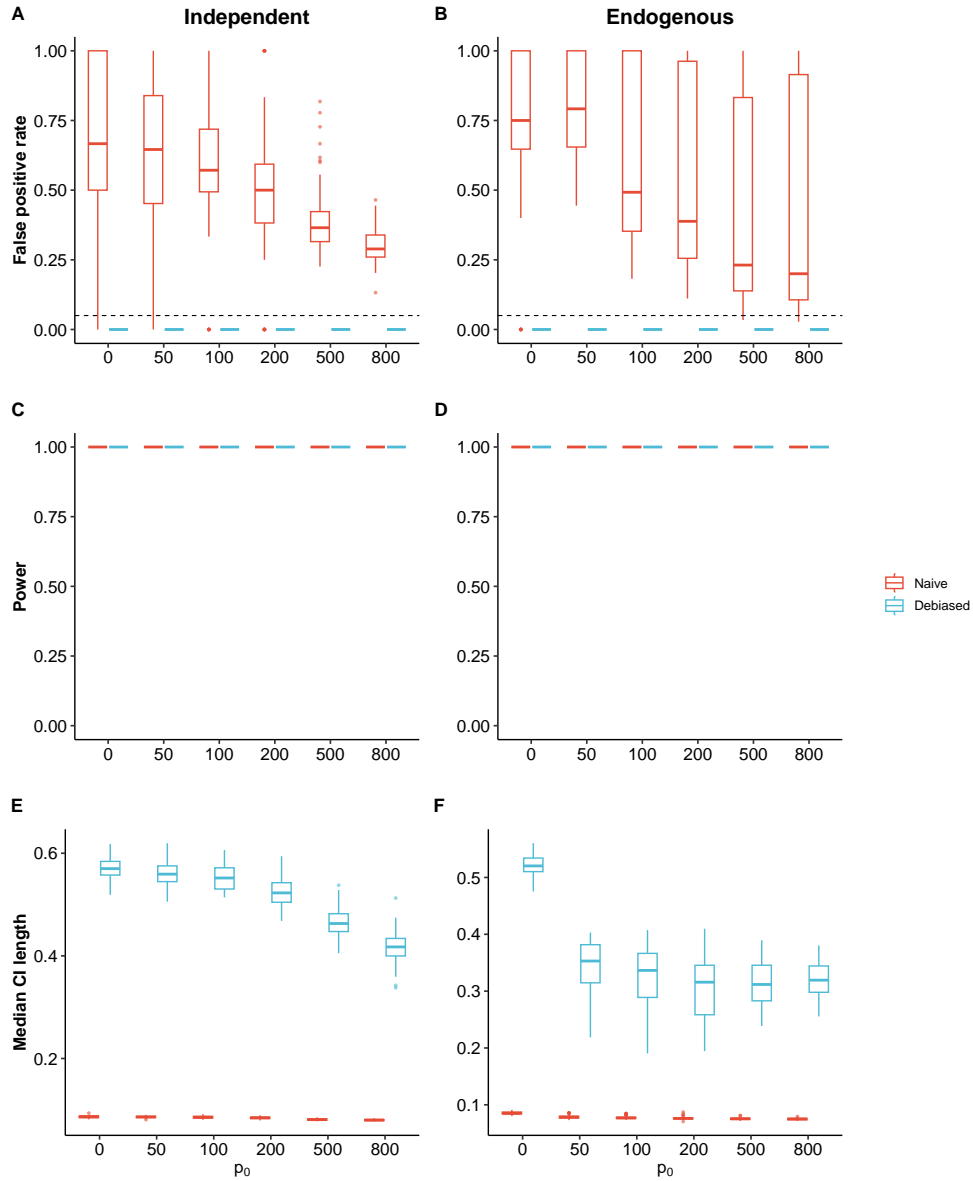


Figure S8: False positive rate, power, and median 95% CI length for Gaussian mixture random intercepts, with variables selected from SHEL.

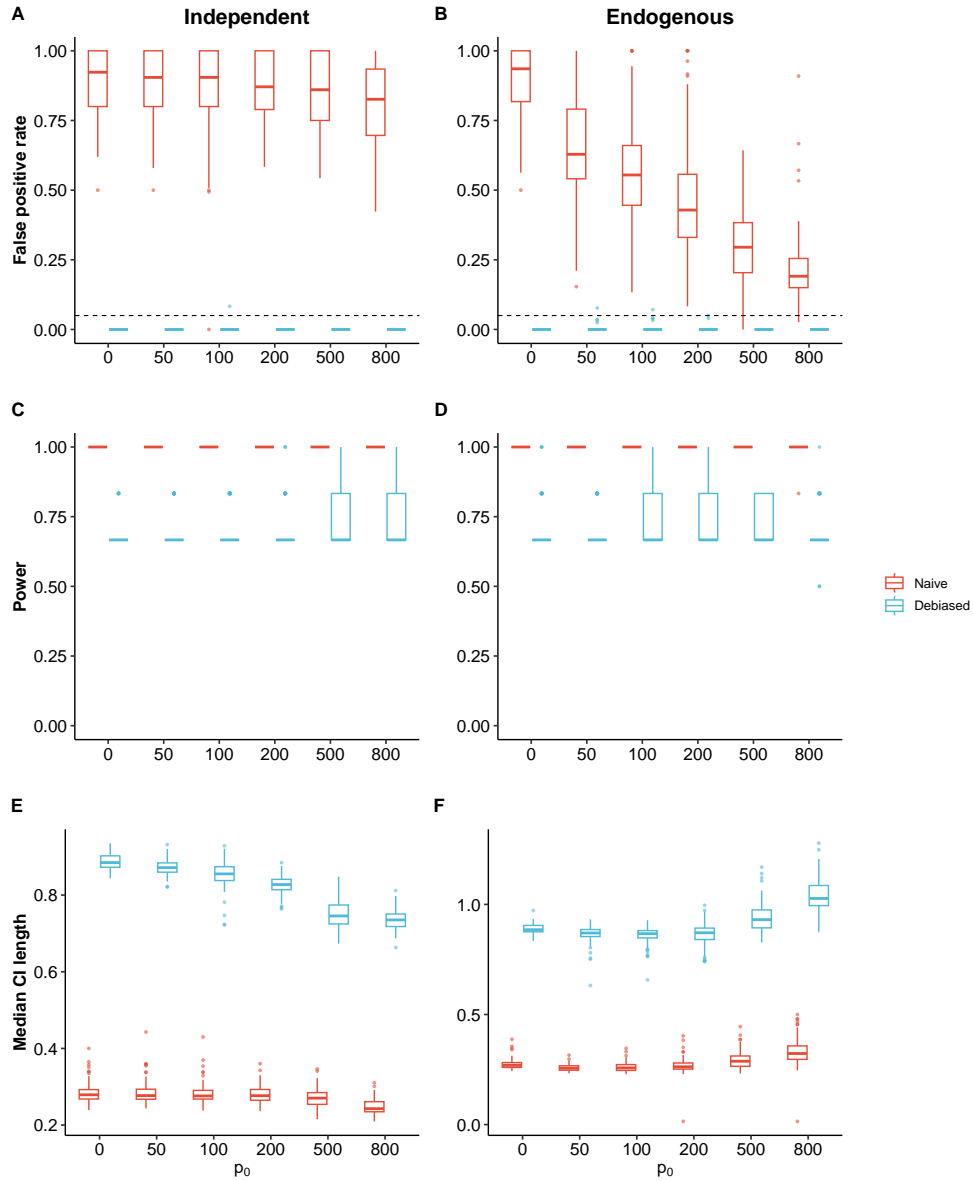


Figure S9: False positive rate, power, and median 95% CI length for Gaussian mixture random intercepts, with variables selected from GSHEL.

F Results for real data analysis

Table S2: Biological categories of the 37 genes selected by GSHEL.

Category	Selected Genes	Biological Relevance
G-MDSC markers (3)	<i>S100A12*</i> , <i>CD177</i> , <i>MCEMP1</i>	Core NMF5 markers; top features in original LASSO model
Longitudinal signal (1)	<i>SERPINB2*</i>	Diverging trajectory between severe and non-severe patients
Neutrophil chemotaxis (1)	<i>CXCL2</i>	Neutrophil migration pathway enriched in severe disease
MHC class II (2)	<i>HLA-DMA</i> , <i>HLA-DMB</i>	Enriched in non-severe patients
Interferon response (4)	<i>RARRES3*</i> , <i>IRF2BP2</i> , <i>UPP1</i> , <i>CTSW</i>	Interferon pathways enriched in infection and associated with severity
Metabolism / ROS (3)	<i>NQO2</i> , <i>GPAT4</i> , <i>ALDH1A1</i>	Metabolic pathways associated with severe disease
Myeloid differentiation (2)	<i>HOTAIRM1</i> , <i>PDE4D</i>	Known roles in neutrophil development and activation
Humoral immunity (2)	<i>IGHM</i> , <i>IGLVI-70*</i>	Humoral immune responses associated with severity
Other protein-coding (11)	<i>CCR3</i> , <i>TSPAN2*</i> , <i>TDRD9*</i> , <i>USP11</i> , <i>METTL7B</i> , <i>COA4</i> , <i>YBEY</i> , <i>MLH3</i> , <i>RPGRIP1*</i> , <i>NOV</i> , <i>AC008763.3*</i>	Immune signaling, regulation, and cell metabolism
Non-coding / unannotated (8)	<i>LINC00877</i> , <i>RPL21P44</i> , <i>AC105749.1</i> , <i>AC037198.2*</i> , <i>AC108134.3</i> , <i>AC023906.5</i> , <i>AC009303.4</i> , <i>ENSG00000288064*</i>	Functional interpretation limited

*Individually significant ($p < 0.05$) by the debiased GSHEL.

Ensembl IDs are retained for genes without established gene symbols.

References

- Belloni, A., Chernozhukov, V., and Wang, L. (2014). Pivotal estimation via square-root lasso in nonparametric regression. *Annals of Statistics*, 42(2):757–788.
- Berk, R., Brown, L., Buja, A., Zhang, K., and Zhao, L. (2013). Valid post-selection inference. *The Annals of Statistics*, 41(2):802–837.

- Bickel, P. J., Ritov, Y., and Tsybakov, A. B. (2009). Simultaneous analysis of lasso and dantzig selector. *Annals of Statistics*, 37(4):1705–1732.
- Billingsley, P. (2013). *Convergence of probability measures*. John Wiley & Sons.
- Bunea, F., Tsybakov, A. B., and Wegkamp, M. (2007). Sparsity oracle inequalities for the lasso. *Electronic Journal of Statistics*, 1:169–194.
- Chen, Y., Tang, C. F., Chiou, S. H., and Chen, M. (2026). Variable selection for stratified sampling designs in semiparametric accelerated failure time models with clustered failure times. *Journal of Multivariate Analysis*, page 105656.
- D’Alessandro, M. and Thoresen, M. (2025). Methods of selective inference for linear mixed models: a review and empirical comparison. *arXiv preprint arXiv:2503.09812*.
- Deaner, B. (2021). Many proxy controls. *arXiv preprint arXiv:2110.03973*.
- Fan, J. and Li, R. (2001). Variable selection via nonconcave penalized likelihood and its oracle properties. *Journal of the American Statistical Association*, 96(456):1348–1360.
- Fan, Y. and Li, R. (2012). Variable selection in linear mixed effects models. *The Annals of Statistics*, 40(4):2043–2068.
- Fithian, W., Sun, D., and Taylor, J. (2014). Optimal inference after model selection. *arXiv preprint arXiv:1410.2597*.
- Grilli, L. and Rampichini, C. (2011). The role of sample cluster means in multilevel models. *Methodology*, 7(4).
- Hansen, C. and Liao, Y. (2019). The factor-lasso and k-step bootstrap approach for inference in high-dimensional economic applications. *Econometric Theory*, 35(3):465–509.

- Hastie, T., Tibshirani, R., and Friedman, J. (2009). The elements of statistical learning.
- Heiling, H. M., Rashid, N. U., Li, Q., and Ibrahim, J. G. (2024). glmmpen: high dimensional penalized generalized linear mixed models. *The R journal*, 15(4):106.
- Hui, F. K., Müller, S., and Welsh, A. (2017). Hierarchical selection of fixed and random effects in generalized linear mixed models. *Statistica Sinica*, pages 501–518.
- Kuchibhotla, A. K., Kolassa, J. E., and Kuffner, T. A. (2022). Post-selection inference. *Annual Review of Statistics and Its Application*, 9:505–527.
- LaSalle, T. J., Gonye, A. L., Freeman, S. S., Kaplonek, P., Gushterova, I., Kays, K. R., Manakongtreecheep, K., Tantivit, J., Rojas-Lopez, M., Russo, B. C., et al. (2022). Longitudinal characterization of circulating neutrophils uncovers phenotypes associated with severity in hospitalized covid-19 patients. *Cell Reports Medicine*, 3(10).
- Le Duy, V. N. and Takeuchi, I. (2021). Parametric programming approach for more powerful and general lasso selective inference. In *International conference on artificial intelligence and statistics*, pages 901–909. PMLR.
- Lee, J. D., Sun, D. L., Sun, Y., and Taylor, J. E. (2016). Exact post-selection inference, with application to the lasso. *The Annals of Statistics*, 44(3):907–927.
- Li, G., Lai, P., and Lian, H. (2015). Variable selection and estimation for partially linear single-index models with longitudinal data. *Statistics and Computing*, 25(3):579–593.
- Meinshausen, N. and Bühlmann, P. (2006). High-dimensional graphs and variable selection with the lasso. *The Annals of Statistics*, 34(3):1436–1462.
- Muff, S., Held, L., and Keller, L. F. (2016). Marginal or conditional regression models for correlated non-normal data? *Methods in Ecology and Evolution*, 7(12):1514–1524.

- Mulayoff, R. and Michaeli, T. (2019). On the minimal overcompleteness allowing universal sparse representation. *IEEE Transactions on Information Theory*, 65(6):3585–3599.
- Negahban, S., Yu, B., Wainwright, M. J., and Ravikumar, P. (2009). A unified framework for high-dimensional analysis of m -estimators with decomposable regularizers. *Advances in neural information processing systems*, 22.
- Rinaldo, A., Wasserman, L., G'Sell, M., Lei, J., and Tibshirani, R. (2019). Bootstrapping and sample splitting for high-dimensional, assumption-free inference. *The Annals of Statistics*, 47(6):3438–3469.
- Taylor, J. and Tibshirani, R. (2018). Post-selection inference for l_1 -penalized likelihood models. *Canadian Journal of Statistics*, 46(1):41–61.
- Tibshirani, R. (1996). Regression shrinkage and selection via the lasso. *Journal of the Royal Statistical Society: Series B (Methodological)*, 58(1):267–288.
- Tibshirani, R. J., Taylor, J., Lockhart, R., and Tibshirani, R. (2016). Exact post-selection inference for sequential regression procedures. *Journal of the American Statistical Association*, 111(514):600–620.
- Tutz, G. and Groll, A. (2013). Likelihood-based boosting in binary and ordinal random effects models. *Journal of Computational and Graphical Statistics*, 22(2):356–378.
- Van de Geer, S., Bühlmann, P., Ritov, Y., and Dezeure, R. (2014). On asymptotically optimal confidence regions and tests for high-dimensional models. *The Annals of Statistics*, 42(3):1166–1202.
- Van de Geer, S. A. (2019). High-dimensional generalized linear models and the lasso. *Annals of Statistics*, 36(2):614–645.

- Wainwright, M. J. (2019). *High-dimensional statistics: A non-asymptotic viewpoint*, volume 48. Cambridge university press.
- Wang, L., Zhou, J., and Qu, A. (2012). Penalized generalized estimating equations for high-dimensional longitudinal data analysis. *Biometrics*, 68(2):353–360.
- Xu, P., Wu, P., Wang, Y., and Zhu, L. (2010). A gee based shrinkage estimation for the generalized linear model in longitudinal data analysis. Technical report, Technical report, Department of Mathematics, Hong Kong Baptist University.
- Ye, S., Rakshe, S., and Liang, Y. (2025a). High-dimensional statistical inference and variable selection using sufficient dimension association. *arXiv preprint arXiv:2410.19031v2*.
- Ye, S., Rakshe, S., and Liang, Y. (2026). High-dimensional statistical inference and variable selection using sufficient dimension association. *Journal of the American Statistical Association*, (accepted):1–24.
- Ye, S., Yu, T., Caroff, D. A., Huang, S. S., Zhang, B., and Wang, R. (2025b). Variable selection in modelling clustered data via within-cluster resampling. *Canadian Journal of Statistics*, 53(1):e11824.
- Zeger, S. L., Liang, K.-Y., and Albert, P. S. (1988). Models for longitudinal data: a generalized estimating equation approach. *Biometrics*, pages 1049–1060.
- Zhang, C.-H. and Zhang, S. S. (2014). Confidence intervals for low dimensional parameters in high dimensional linear models. *Journal of the Royal Statistical Society Series B: Statistical Methodology*, 76(1):217–242.
- Zhang, H. and Jia, J. (2022). Elastic-net regularized high-dimensional negative binomial regression. *Statistica Sinica*, 32(1):181–207.